Electronic Supplementary Material (ESI) for Journal of Materials Chemistry A.

Supplementary Information

A Cradle-to-Cradle Approach for Successive Upcycling of Polyethylene to Polymer Electrolytes to Organic Acids

Jerald Y. Q. Teo,†[a] Ming Yan Tan,†[a] Dorsasadat Safanama,[a] Sheau Wei Chien,[a] Yixuan Jiang,[a,e] Lewis Queh,[b] Tristan T. Y. Tan,[a] Ding Ning,[a] Derrick W. H. Fam[a,c,d*] and Jason Y. C. Lim[a,e*]

a. Institute of Materials Research and Engineering (IMRE), Agency for Science, Technology and Research (A*STAR), 2 Fusionopolis Way, Innovis #08-03, Singapore 138634, Republic of Singapore. E-mail: jason_lim@imre.a-star.edu.sg; derrickfamwh@imre.a-star.edu.sg

b. Institute of Sustainability for Chemicals, Energy and Environment (ISCE2), Agency for Science, Technology and Research (A*STAR), 1 Pesek Road, Jurong Island, Singapore 627833, Republic of Singapore.

c. School of Materials Science and Engineering, Nanyang Technological University, 50 Nanyang Ave, Singapore 639798, Singapore

d. Department of Mechanical Engineering, College of Design and Engineering, National University of Singapore, 9 Engineering Drive 1, Block EA #07-08, Singapore 117575, Singapore

e. Department of Materials Science and Engineering, National University of Singapore (NUS), 9 Engineering Drive 1, Singapore 117576, Singapore

† These authors contributed equally to the manuscript.

S1. Experimental

S1.1 Materials and Methods

All chemicals were used as received. Polyethylene (PE, M_n ~7.7 kDa, M_w ~35 kDa, PDI = 4.55), 1,2,4-trichlorobenzene (TCB, ≥ 99%), 1,1,2,2-tetrachloroethane (TCE, ≥ 98%), 1,2-dichloroethane (DCE, ≥ 99%), polycaprolactone (PCL, average M_n 80 kDa), *N*-hydroxytetrachlorophthalimide (Cl_4-NHPI), *N*-hydroxysuccinimide (NHS, 98%), TEMPO (99%), tetrafluorophthalic anhydride (97%), 3,6-difluoro phthalic anhydride (97%), 3-fluorophthalic anhydride (95%), 4-fluorophthalic anhydride (97%), 4-nitro phthalic anhydride (92%), tetrabromophthalic anhydride (98%), 1,2,4-benzenetricarboxylic anhydride (97%), 3,3',4,4'-benzophenonetetracarboxylic dianhydride (98%), sodium acetate (≥ 99%), toluene (anhydrous, 99.8%), glacial acetic acid (≥ 99%), hydroxylamine hydrochloride (98%), ε-caprolactone (97%), tin(II) 2-ethylhexanoate (stannous octoate, 92.5%) and (3*S*)-*cis*-3,6-dimethyl-1,4-dioxane-2,5-dione (*L*-lactide, 98%) were all purchased from Sigma-Aldrich. *N*-hydroxyphthalimide (NHPI, > 99%) and lithium *bis*(trifluoromethanesulfonyl)imide (LiTFSI, > 98%) were sourced from Tokyo Chemical Industry (TCI). 1-hydroxybenzotriazole (HOBt) and 2,6-*di*-*tert*-butyl-4-methylphenol (BHT, ≥ 99%) were obtained from Alfa Aesar, while *N*,*N*',*N*''-trihydroxyisocyanuric acid (THICA, 95%) was obtained from Angene International Ltd. Methanol (A.C.S. grade) and diethyl ether (AR grade, 99%) were supplied by J.T. Baker® and VWR respectively. Chloroform-*d* ($CDCl_3$, 99.8%), 1,1,2,2-tetrachloroethane-d_2 (TCE-d_2, 99.5%) and dimethyl sulfoxide-d_6 (DMSO-d_6, 99.9%) were purchased from Cambridge Isotope Laboratories. High-density polyethylene (HDPE) resins used for polymer electrolyte synthesis were sourced from SCG Chemicals.

The presence of functional groups in the oxidised PEs was identified by ^{1}H and ^{13}C nuclear magnetic resonance (NMR) in TCE-d_2 at 80 °C using a JEOL 500 MHz spectrometer (Tokyo, Japan). These were further verified *via* Fourier-transform infrared (FTIR) spectroscopy using a Bruker VERTEX 80v spectrometer (Karlsruhe, Germany) in the attenuated total reflectance mode from 4000 to 400 cm^{-1}. X-ray photoelectron spectroscopic (XPS) analysis was performed using a Thermo Scientific Theta Probe Angle-Resolved XPS spectrometer (Waltham, US). Monochromatic Al K_α X-ray source (hv = 1486.7 eV) with spot size of 400 µm was employed, and photoelectrons were collected at a take-off angle of 50° with respect to the surface normal. Survey spectra were acquired with pass energy of 200 eV and step size of 1 eV for elemental identification. High-resolution scans were acquired with pass energy of 40 eV and step size of 0.1 eV for chemical state identification.

Thermogravimetric analysis (TGA) was conducted using TGA Q500 (TA Instruments) under N_2 with a flow rate of 60 mL/min. Each sample was heated from room temperature to 700 °C at a rate of 20 °C/min. Differential scanning calorimetry (DSC) was carried out using TA Instruments PDSC Q100 at a heating rate of 20 °C/min over a temperature range of −50 to 140 °C for PE-PLA and 190 °C for PE-PCL. Each sample was prepared and crimp sealed in an aluminium hermetic pan and lid inside a glovebox. The polymer melting temperature (T_m) was collected from the second cycle of heating.

Gel-permeation chromatography (GPC) was performed at 160 °C in TCB using an Agilent 1260 Infinity II High Temperature GPC system. TCB stabilised with 250 ppm of BHT (10 mL) was added to 20 mg of sample in a 20-mL vial. The samples were dissolved by heating to 160 °C with shaking for 2 hours on an Agilent high-temperature sample preparation system. The solutions were then pipetted into 2-mL vials using a heated pipette with filter from the sample preparation system, followed by crimping of the vial caps. For analysis, the GPC system was equipped with 2 columns of Agilent PLgel Olexis (300 mm x 7.5 mm, 13 µm) connected in series, as well as a refractive index detector. The column oven was maintained at 160 °C with a flow rate of 1.0 mL/min and a sample injection volume of 100 µL. The calibration standard in use is Agilent PS-H EasiVial.

LC-ESI-MS analysis of the dicarboxylic acids obtained from PE-PCL, PCL and PE-OH degradation was performed using an Agilent 6125 single quadrupole LC/MSD with Infinity II HPLC. Chromatographic separation was attempted using Hi-Plex H column (4.6 x 250 mm) coupled with its corresponding PL Hi-Plex H guard column (7.7 × 50 mm). The column temperature was maintained at 40 °C, and the flow rate and injection volume were set at 0.2 mL/min and 5 µL respectively. Mobile phase used for the analysis was 0.01% aqueous formic acid/acetonitrile = 80/20. The LCMS system was equipped with an ESI source operating in negative-ion detection mode.

The morphology of the prepared electrolytes was inspected using a scanning electron microscope (JEOL JSM 6700F) operating at accelerating voltage of 5 kV. X-ray diffraction (XRD) data of the polymers was collected using a Bruker D8 advance diffractometer equipped with Cu-K_α radiation (1.54 Å) with step size of 0.02° and a scan rate of 1 s/step.

S1.2 Polyethylene Functionalisation

Aerobic oxidation of PE

Polyethylene (500 mg) and Cl_4-NHPI (134 mg, 2.5 mol% w.r.t. ethylene repeating units) were dissolved in TCB (13 mL) in a round-bottomed flask. The reaction mixture was stirred and refluxed at 120 °C for 24 hours in air. After the reaction, the crude reaction mixture was poured into vigorously-stirred methanol (150 mL) to afford a suspension, which was then filtered, rinsed with methanol, and dried in vacuo to obtain the oxidised PE as a powder (typical recovered yields > 80%). ^{1}H NMR of oxidised PE ($C_2D_2Cl_4$, 80 °C) δ/ ppm: 3.92 (*quint*, H adjacent to C–Cl); 3.61 (*br*, H adjacent to C–OH); 2.40 (*t*, C_α–H of ketones); 2.32 (*t*, C_α–H of carboxylic acids); 0.7–1.8 (*m*, CH_2s of PE). ^{13}C NMR of oxidised PE ($C_2D_2Cl_4$, 80 °C) δ/ ppm: 211.3 (ketone C=O); 42.9 (C_α of ketones); 38.0–7.7 (alkyl branches of PE).

Reduction of oxidised PE

Oxidised PE (4.50 g) was dissolved in toluene (100 mL) in a round-bottomed flask at 100 °C. After the polymer had completely dissolved, the solution was cooled to 60 °C before tetrahydrofuran (70 mL) was added. Sodium borohydride (0.94 g, 20 wt% of oxidised PE) was added slowly portionwise, and the reaction mixture was then refluxed at 90 °C for 24 hours. After the reaction, the reaction mixture was poured into vigorously-stirred methanol (400 mL) to afford a suspension, which was then filtered, rinsed with methanol, and dried in vacuo to obtain the PE-OH precursor as a powder (> 90% recovered yield, ~2.3% OH functionalisation). ^{1}H NMR of PE-OH precursor ($C_2D_2Cl_4$, 80 °C) δ/ ppm: 3.61 (*br*, H adjacent to C–OH); 2.32 (*t*, C_α–H of carboxylic acids); 2.1–0.8 (*m*, CH_2s of PE).

S1.3 Synthesis of Polymer Electrolytes

Synthesis of PE-PCL copolymer

PE-OH precursor (2.01 g) was loaded into a 200-mL Schlenk flask equipped with a magnetic stir bar. The flask was degassed and refilled with argon gas thrice. Under argon, anhydrous toluene (25 mL) was added into the flask through the rubber septum using a syringe and needle. Stannous octoate (2.0 mL, 10 mol% w.r.t. ε-caprolactone) was dissolved in anhydrous toluene (5 mL) in a glass vial and the solution was transferred into the reaction flask. The vial was rinsed with anhydrous toluene (3 mL), which was then combined with the reaction mixture. Whilst stirring, ε-caprolactone (7.0 mL, 38 equiv. w.r.t. %OH functionalisation on PE) was added to the reaction mixture. The ring-opening polymerisation reaction was allowed to proceed for 42 hours at 110 °C under inert atmosphere. The reaction mixture was cooled to 50 °C before quenching with acetone (100 mL). After leaving to stir at 50 °C for 30 minutes, the crude mixture was slowly poured into vigorously-stirred methanol (200 mL) to afford a suspension, which was then filtered, rinsed with methanol, and dried in vacuo to obtain the PE-PCL polymer electrolyte as a powder. Yield = 5.64 g. ^{1}H NMR of PE-PCL ($CDCl_3$) δ/ ppm: 4.86 [*quint*, C***H***–O–C(O)]; 4.06 [*t*, C***H$_2$ε***–OC(O)]; 3.65 (*t*, C***H$_2$ε'***–OH); 2.30 (*t*, O–C(O)C***H$_2$α***); 1.70–1.60 [*m*, C***H$_2$β***–CH_2C***H$_2$δ***–CH_2–OC(O)]; 1.43–1.35 [*m*, CH_2C***H$_2$γ***–CH_2CH_2–OC(O)]; 1.31–0.77 (*m*, CH_2s of PE). ^{13}C NMR of PE-PCL ($C_2D_2Cl_4$, 80 °C) δ/ ppm: 173.4 (ester C=O); 64.2 (ester C–O); 34.3–24.7 (alkyl chains of PE and PCL).

Synthesis of PE-PLA copolymer

PE-OH precursor (2.05 g) was loaded into a 200-mL Schlenk flask equipped with a magnetic stir bar. The flask was degassed and refilled with argon gas thrice. Under argon, anhydrous toluene (25 mL) was added into the flask through the rubber septum using a syringe and needle. Stannous octoate (0.5 mL, 5 mol% w.r.t. *L*-lactide) was dissolved in anhydrous toluene (5 mL) in a glass vial and the solution was transferred into the reaction flask. The vial was rinsed with anhydrous toluene (3 mL), which was then combined with the reaction mixture. Whilst stirring, *L*-lactide (4.55 g, 19 equiv. w.r.t. %OH functionalisation on PE) was added to the reaction mixture. The ring-opening polymerisation reaction was allowed to proceed for 42 hours at 110 °C under inert atmosphere. The reaction mixture was cooled to 50 °C before quenching with acetone (100 mL). After leaving to stir at 50 °C for 30 minutes, the crude mixture was slowly poured into vigorously-stirred methanol (200 mL) to afford a suspension, which was then filtered, rinsed with methanol, and dried in vacuo to obtain the PE-PLA polymer electrolyte as a powder. Yield = 5.42 g. ^{1}H NMR of PE-PLA ($CDCl_3$) δ/ ppm: 5.18–5.14 [*q*, O–C(O)C***H***(CH_3)–OC(O)]; 4.88 [*quint*, C***H***–O–C(O)]; 4.37–4.33 (*q*, O–C(O)C***H***(CH_3)–OH); 1.59–1.57 (*d*, O–C(O)CH(C***H$_3$***)–O); 1.35–0.77 (*m*, CH_2s of PE).

S1.4 Procedures for Polymer Electrolyte Testing

Preparation of PE-based films

Varying amounts of PE-based polymers, LiTFSI salt, and/or EMITFSI ionic liquid were added to anhydrous 2-methyltetrahydrofuran (2-MeTHF) and stirred at 80 °C until all precursors were fully dispersed/dissolved. The resultant solution was dried at 80 °C under vacuum overnight to fully remove the solvent and obtain a dry paste. The PE precursors, PE-PCL and PE-PLA paste were subsequently hot-pressed into films in a two-step process under different temperatures and pressures. PE-precursors were first kept at 110 °C for 30 min to allow the paste to melt, followed by a pressure of 5 bar for 5 min. PE-PCL and PE-PLA samples were both preheated at 90 °C for 10 min; thereafter, a pressure of 20 bar for 15 min was applied to PE-PCL, and PE-PLA underwent a 5 bar pressure for 10 mins. The resultant films were then rapid cooled to room temperature using an air knife. All films were dried under vacuum at 90 °C for 2 days to remove any trace of moisture, followed by drying at 80 °C under argon overnight. Subsequently, the films were transferred to a Ar-filled glovebox for further characterization and testing.

Electrochemical characterization

Ionic conductivity of the solid and gel polymer electrolytes was characterized using a RHD piezo cell connected to an Autolab FR32 M frequency response analyzer. Discs of 12 mm diameter were cut and mounted onto the cell with symmetric stainless steel current collectors. Impedance spectra were obtained from 100 Hz to 1 MHz in the temperature range of 20 to 80 °C. The ionic conductivities (σ) at each temperature were calculated according to the equation: $\sigma = l/RA$, where *l* is the film thickness, R is the resistance extracted from the Nyquist plot and A is the contact area (diameter = 8 mm) of the electrodes.

Cyclic voltammetry (CV) and linear sweep voltammetry (LSV) were performed to determine the electrochemical stability of the gel polymer electrolyte, with a Li/PE-PCL/stainless steel coin cell. Additional CV was also performed on a Li/PE-PCL/LFP coin cell. The CV and LSV measurements were conducted using Biologic SP-300 at scanning rate of 1mV/s at 60 °C. All cells were assembled in an Ar-filled glovebox (O_2 and H_2O < 0.1 ppm).

Assembly of prototype lithium-ion cells

The Li/PE-PCL/LFP cells were assembled by sandwiching the gel polymer electrolyte between the Li anode and $LiFePO_4$ cathode using a CR2032 coin cell. The loading for active material in the electrode was 52 wt% (≈ 2 mg/cm^2) with 3 wt% of carbon (Super C-65) and 45 wt% PVdF binder and an ion

conducting phase of PEO:LiTFSI (EO:Li ratio of 10:1). All electrodes were dried at 80 °C under vacuum before cell assembly. The cells were charged and discharged at constant current density from 0.1–2C in the voltage range of 2–4 V. All batteries were assembled in an Ar-filled glovebox (O_2 and H_2O < 0.1 ppm). The galvanostatic measurements were carried out using a multichannel battery tester (Neware MHW-25) at 60 °C. The coulombic efficiency (CE) was calculated using the following equation:

CE = (discharge capacity)/(charge capacity) x 100%

S2. Supporting Data for PE Oxidation Experiments

S2.1 Optimisation Experiments

Table S1. Additional optimisation experiments for aerobic PE oxidation[a].

	Solvent	Catalyst	Relative % C=O: OH: COOH: Cl	TF/ %	M_n [c]/ kDa	Đ [c]
1	TCB (Air)	Cl_4-NHPI	63: 10: 9: 18	2.4	2.53	9.7
2	TCB (O_2)	Cl_4-NHPI	67: 11: 9: 13	2.4	1.32	5.8
3	TCB (Argon)	Cl_4-NHPI	-	0	- [d]	- [d]
4	TCB	-	-	0	- [d]	- [d]
5	TCB (48 h)	Cl_4-NHPI	2.7	1.60	7.3	79.5
6	TCB	Cl_4-NHPI (5 mol%)	78: 6: 16: 0 [b]	5.1 [b]	1.06	4.6
7	TCB (100 °C)	Cl_4-NHPI	50: 0: 0: 50	1.2	3.90	9.4
8	TCB (110 °C)	Cl_4-NHPI	47: 9: 6: 38	1.6	2.72	11.2
9	TCB (130 °C)	Cl_4-NHPI	68: 8: 13: 11 [b]	2.8 [b]	2.12	7.0
10	TCB (140 °C)	Cl_4-NHPI	77: 6: 14: 3 [b]	3.4 [b]	1.50	7.1
11	DCE	Cl_4-NHPI	-	-	6.41	13.2

[a] All reactions performed at 120 °C in air for 24 h using 0.5 g PE, 2.5 mol% Cl_4-NHPI w.r.t. ethylene units, 13 mL solvent, and stirring rate of 500 rpm, unless otherwise stated. Values calculated based on C=O, OH, COOH and Cl functionalisation from ^{1}H NMR spectroscopy; [b] Estimated values due to unidentifiable functionalities in the ^{1}H NMR spectra; [c] Determined by high-temperature GPC analysis in TCB, PE starting material having M_n = 6870 Da and Đ = 12.7; [d] Not performed.

Additional control experiments were performed to identify the essential conditions for aerobic PE oxidation by Cl_4-NHPI in TCB. In all cases, carbonyl functionalisation was dominant. The usage of O_2 in air for oxidation (entry 1) gave similar TF values as the use of a pure O_2 atmosphere (entry 2), but resulted in greater extent of polymer chain scission. The necessity for O_2 was confirmed when performing the reaction under argon elicited no PE oxidation (entry 3). We were also able to rule out the possibility that the oxygenated functional groups formed from unsaturated defects on the PE starting material[1] by performing the reaction in the absence of Cl_4-NHPI (entry 4), which afforded no discernible oxidation. Next, the effect of increasing reaction duration was examined by repeating the PE oxidation reaction for 48 h instead of 24 h (entry 5). This only resulted in a modest increase in TF from 2.4 to 2.7, which may be attributed to the spontaneous gradual self-decomposition of the Cl_4-PINO radicals.[2] Doubling the catalyst loading led to a one-fold increase in TF (entry 6) at the expense of more extensive chain scission as evident from the sharp drop in M_n, and an increased COOH functionalisation. Entries 7–10 show that the TF increases with reaction temperature, likely due the increase in rate of *in situ* Cl_4-PINO formation as well as that of C–H bond activation with increasing temperature. Though higher temperatures conferred enhanced carbonyl selectivity, the oxidised PEs had many unidentifiable resonances in their ^{1}H NMR spectra with greater chain scission, suggesting more indiscriminate C–H functionalisation.

Finally, the reaction solvent greatly influenced the outcome of the organocatalysed PE C–H oxidation. Replacing TCB with 1,2-dichloroethane (DCE) (entry 11) resulted in no detectable PE functionalisation. Additionally, we have previously reported that Cl_4-NHPI in 1,1,2,2-tetrachloroethane gave much higher TF value even at a lower reaction temperature of 100 °C, albeit with a loss of functional group selectivity.[3] These results reinforce the active role played by the solvent in the catalytic activity of NHPI catalysts,[4, 5] likely due to its effects on the solvation and reactive lifetime of the Cl_4-PINO radicals.[2]

S2.2 Supporting Spectra

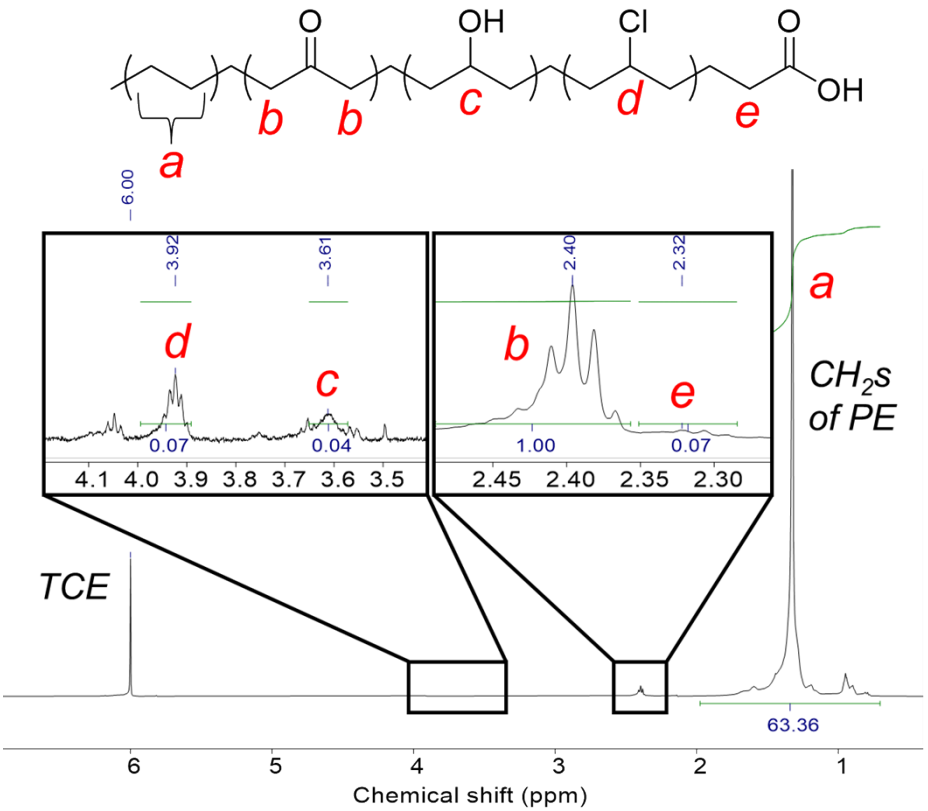

Figure S1. Integrated ^{1}H NMR spectrum ($C_2D_2Cl_4$, 80 °C) of PE product after a 24-hour reaction with 2.5 mol% Cl_4-NHPI in TCB at 120 °C in air.

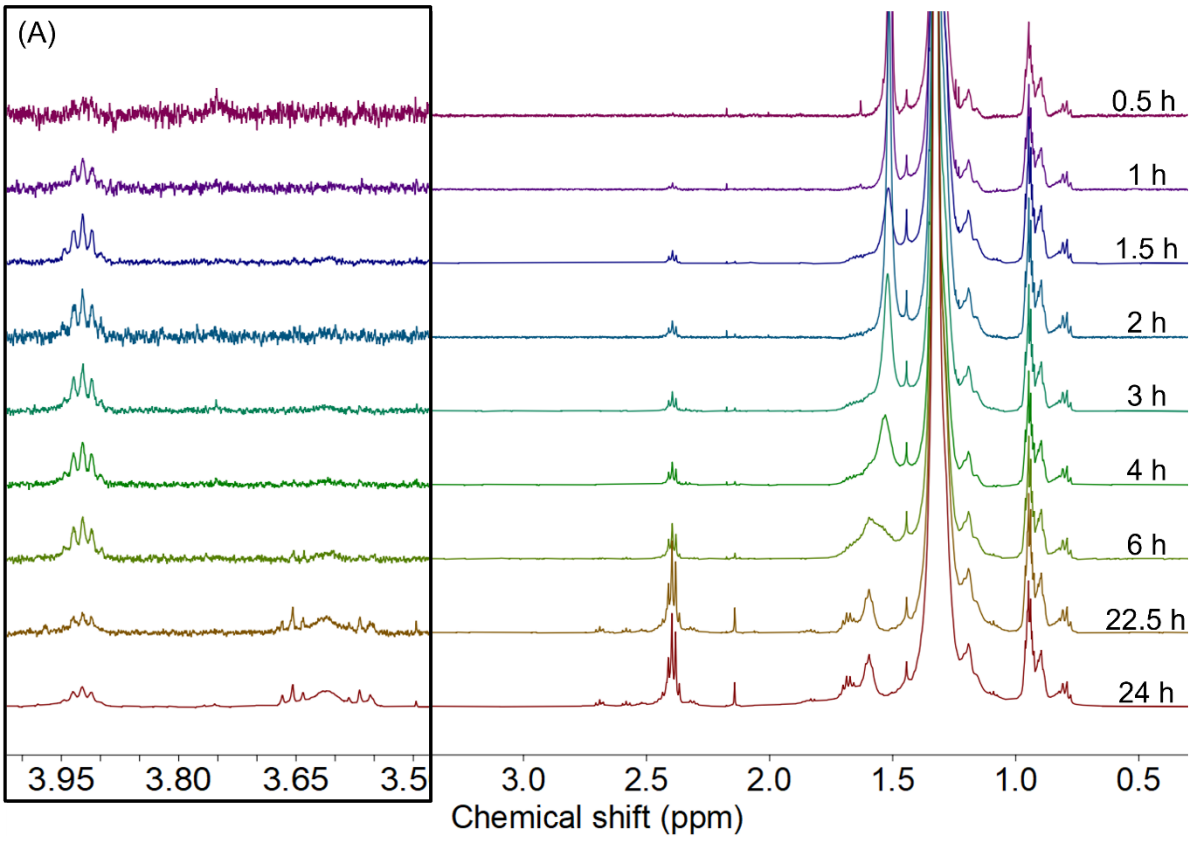

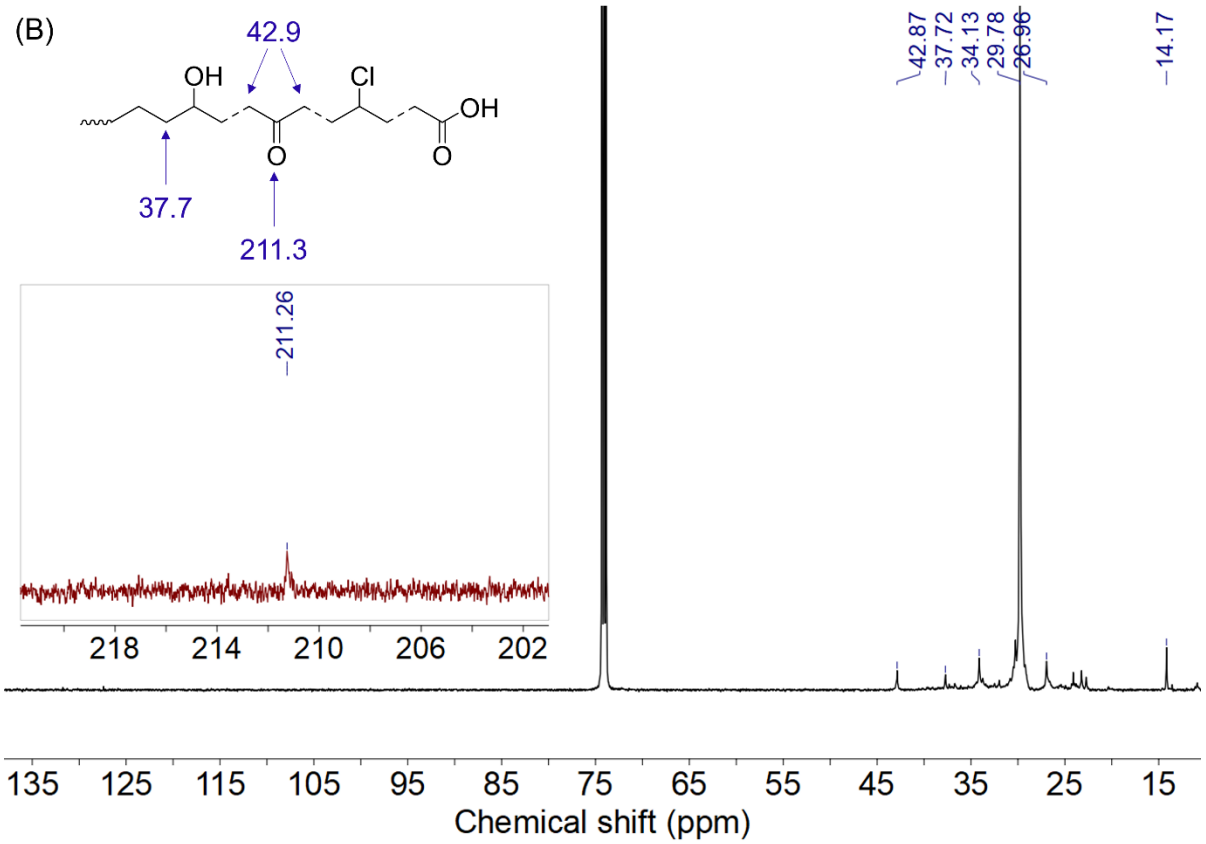

Figure S2. (A) Stacked ^{1}H NMR spectra ($C_2D_2Cl_4$, 80 °C) showing the appearance of signals at 3.92, 3.61, 2.40 and 2.32 ppm arising from -C***H***-Cl-, -C***H***-OH-, -C***H*$_2$-C(O)-C***H***$_2$-, and -C***H***$_2$-COOH, respectively, on PE; (B) ^{13}C NMR spectrum ($C_2D_2Cl_4$, 80 °C) of Cl_4-NHPI-oxidised PE in TCB at 120 °C.

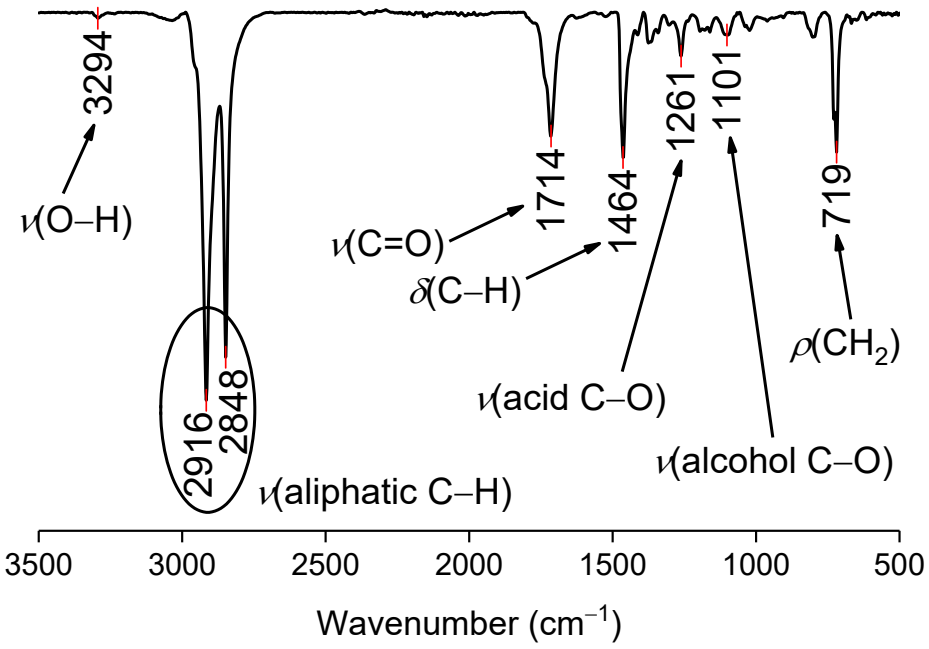

Figure S3. FTIR spectrum of Cl_4-NHPI-oxidised PE in TCB at 120 °C.

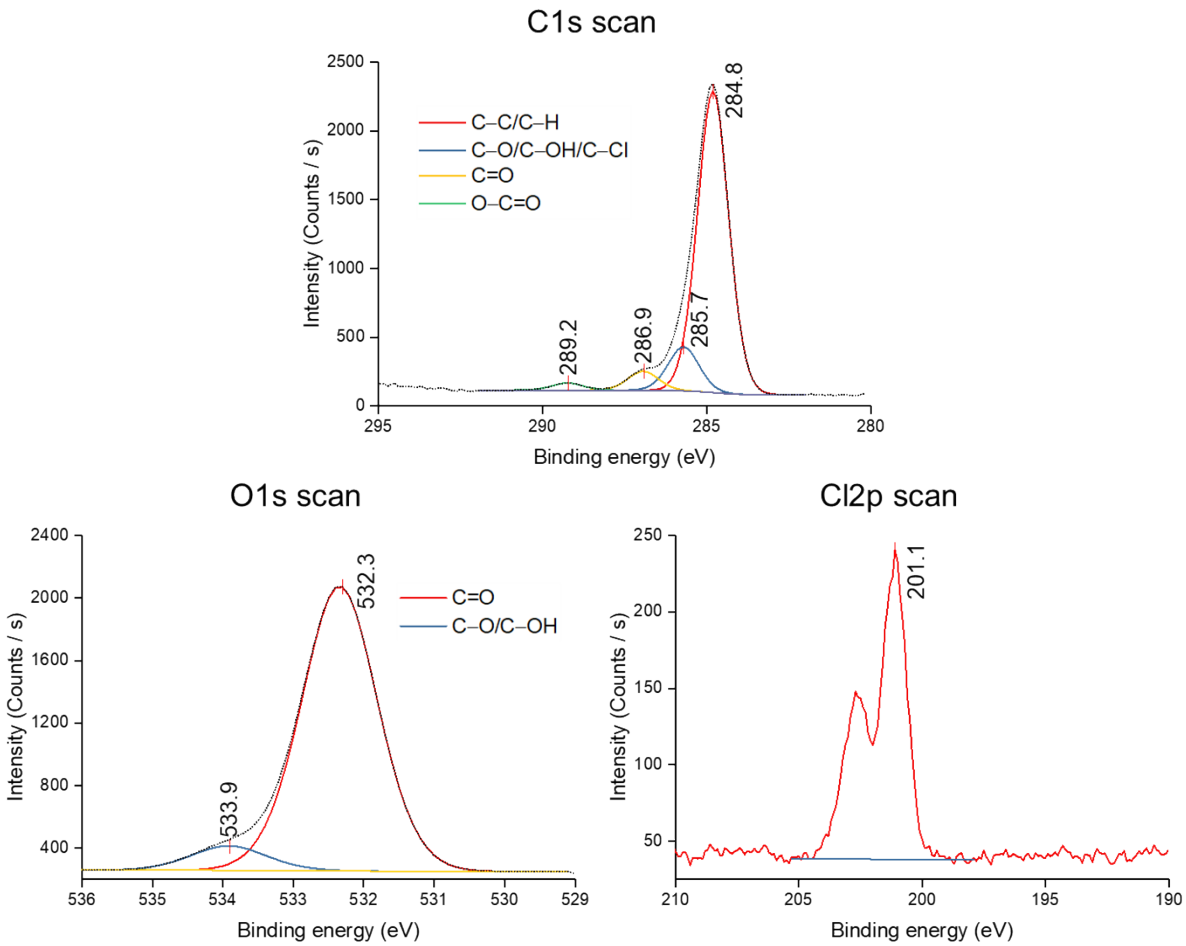

Figure S4. High-resolution C1s, O1s and Cl2p XPS spectra of Cl_4-NHPI-oxidised PE in TCB at 120 °C.

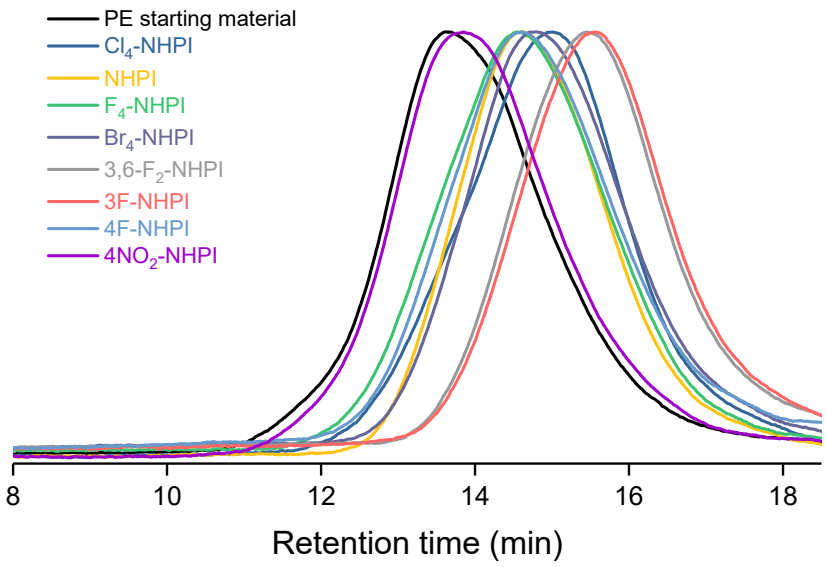

Figure S5. Overlaid normalised GPC chromatograms showing changes in molecular weight distribution of PE before and after oxidation using various NHPI catalysts.

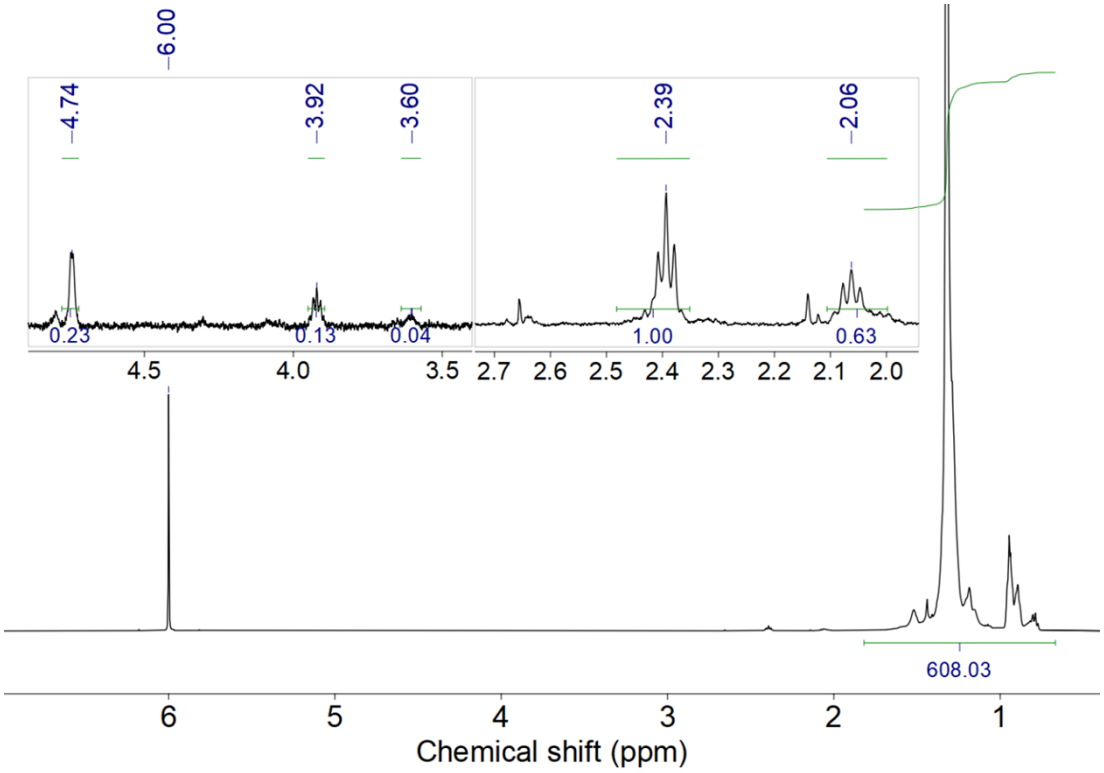

Figure S6. ^{1}H NMR spectrum ($C_2D_2Cl_4$, 80 °C) of the PE product after a 24-hour neat reaction (without TCB solvent) with 2.5 mol% Cl_4-NHPI at 120 °C in air.

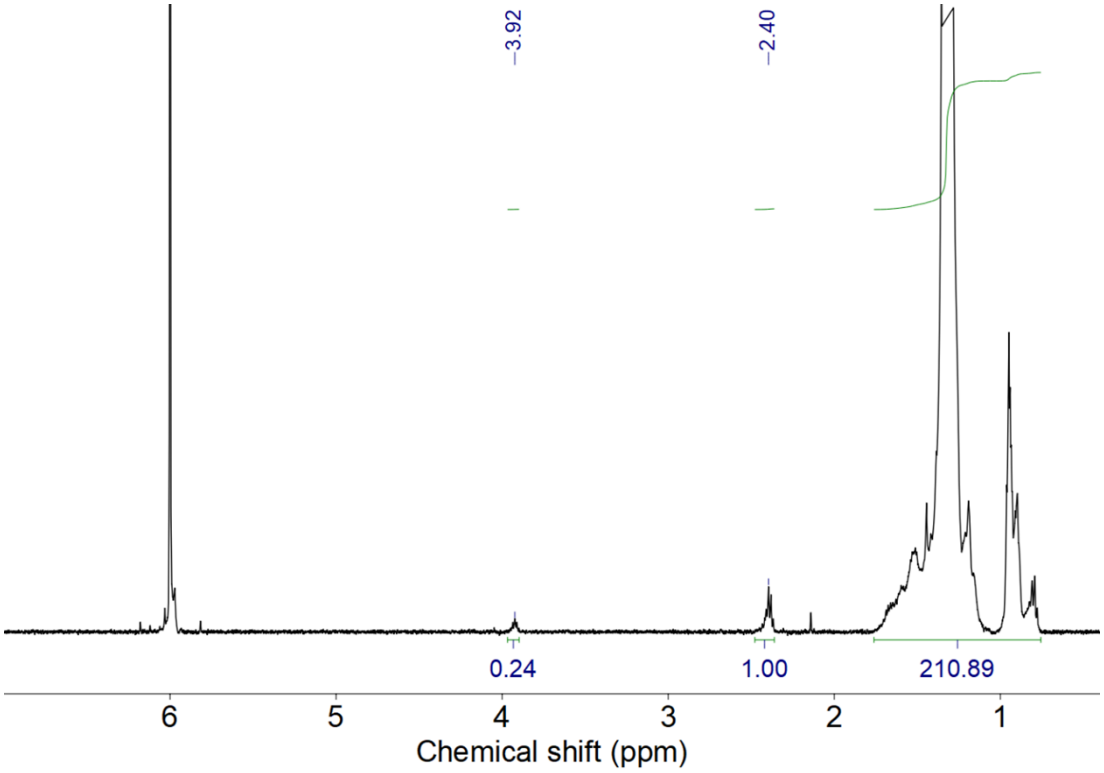

Figure S7. ^{1}H NMR spectrum ($C_2D_2Cl_4$, 80 °C) of PE product after a 24-hour reaction with 2.5 mol% NHPI in TCB at 120 °C in air (Figure 2B).

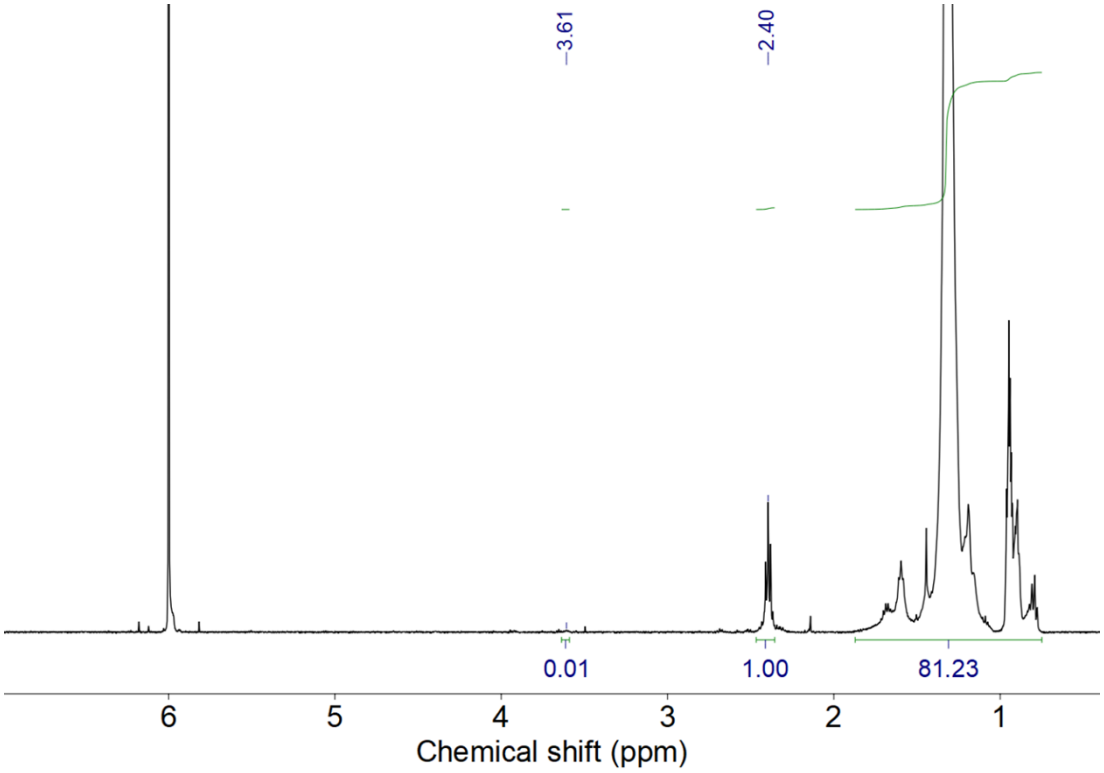

Figure S8. ^{1}H NMR spectrum ($C_2D_2Cl_4$, 80 °C) of PE product after a 24-hour reaction with 2.5 mol% F_4-NHPI in TCB at 120 °C in air (Figure 2B).

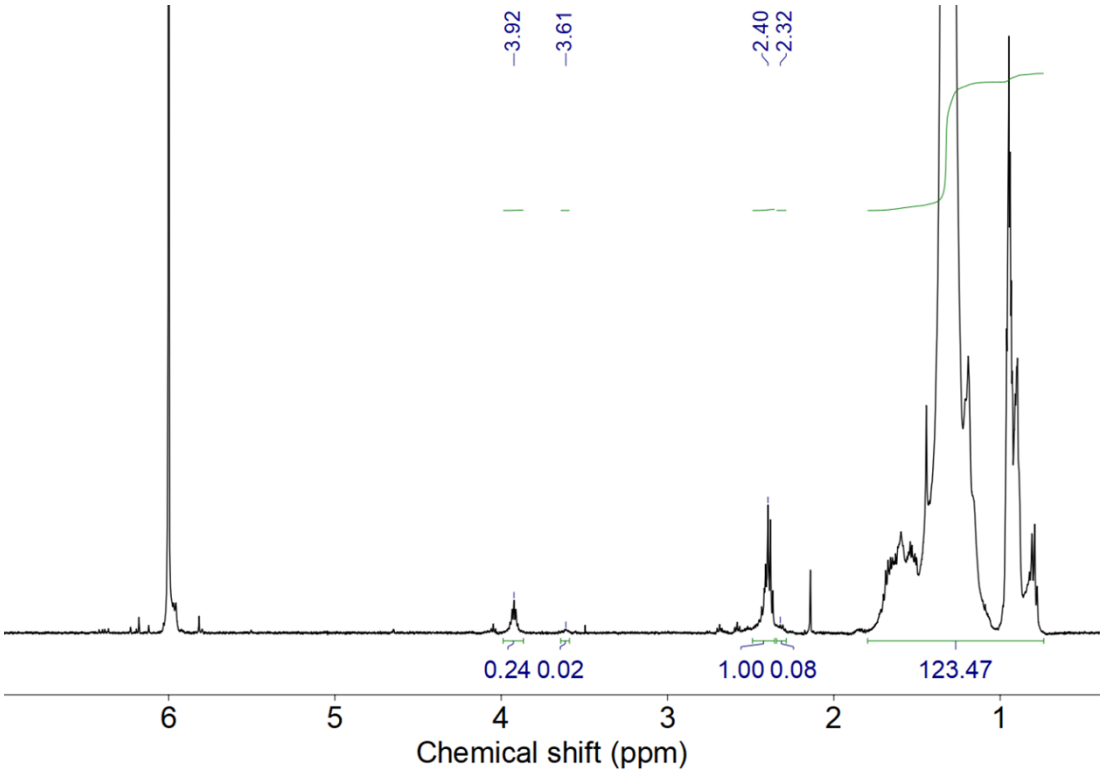

Figure S9. ^{1}H NMR spectrum ($C_2D_2Cl_4$, 80 °C) of PE product after a 24-hour reaction with 2.5 mol% Br_4-NHPI in TCB at 120 °C in air (Figure 2B).

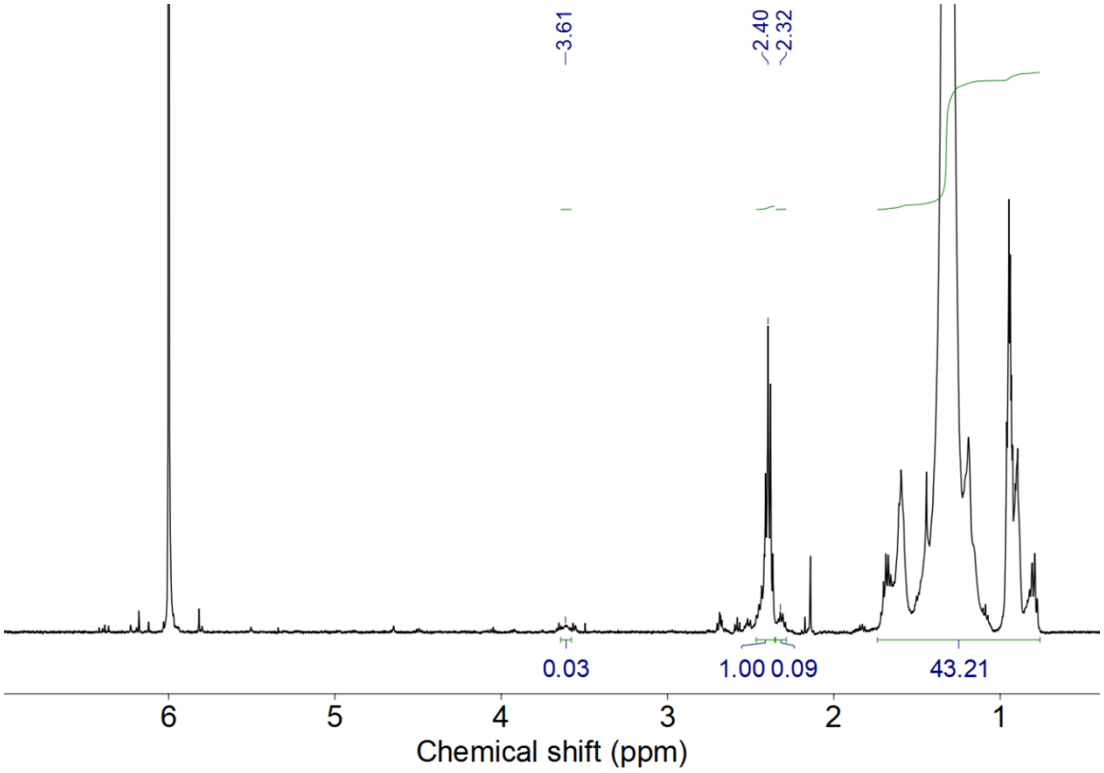

Figure S10. ^{1}H NMR spectrum ($C_2D_2Cl_4$, 80 °C) of PE product after a 24-hour reaction with 2.5 mol% 3,6-F_2-NHPI in TCB at 120 °C in air (Figure 2B).

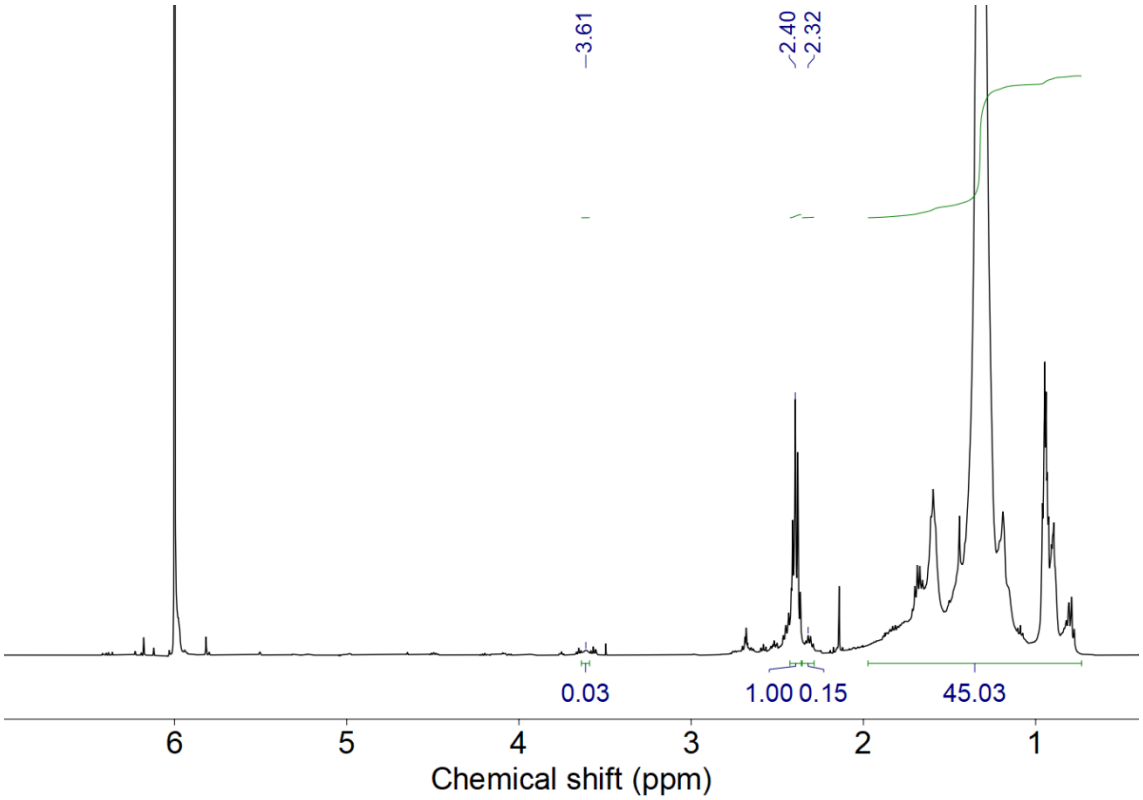

Figure S11. ^{1}H NMR spectrum ($C_2D_2Cl_4$, 80 °C) of PE product after a 24-hour reaction with 2.5 mol% 3-F-NHPI in TCB at 120 °C in air (Figure 2B).

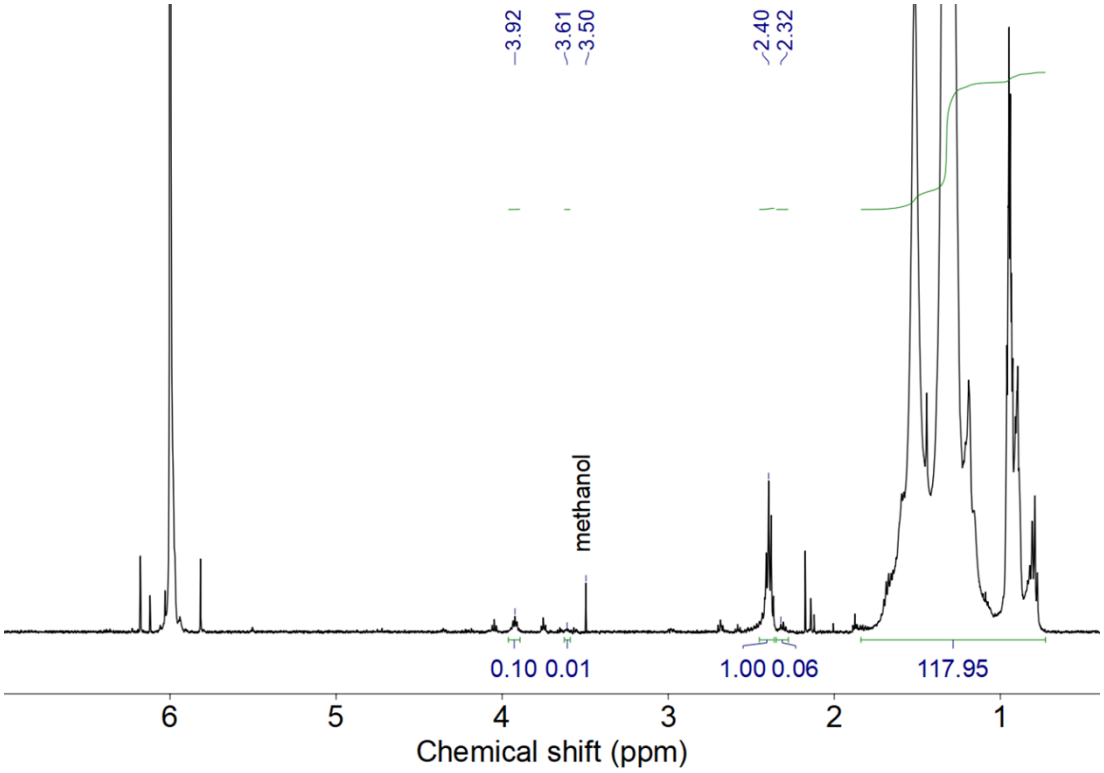

Figure S12. ^{1}H NMR spectrum ($C_2D_2Cl_4$, 80 °C) of PE product after a 24-hour reaction with 2.5 mol% 4-F-NHPI in TCB at 120 °C in air (Figure 2B).

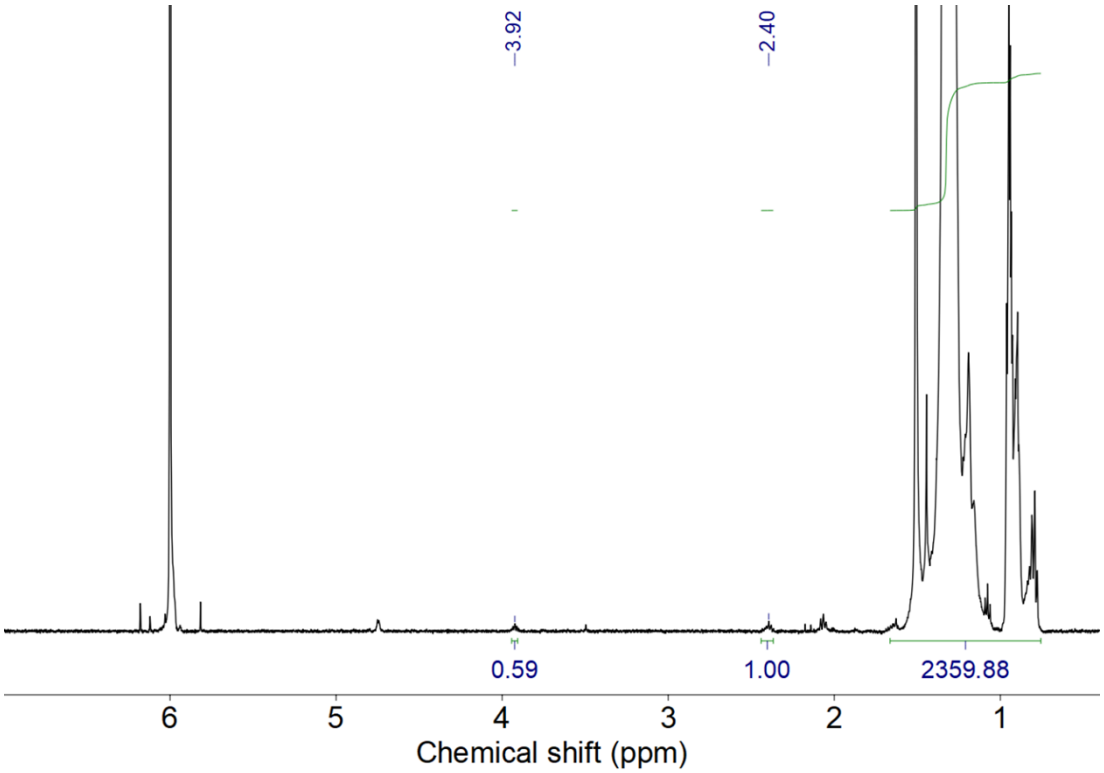

Figure S13. ^{1}H NMR spectrum ($C_2D_2Cl_4$, 80 °C) of PE product after a 24-hour reaction with 2.5 mol% 4-NO_2-NHPI in TCB at 120 °C in air (Figure 2B).

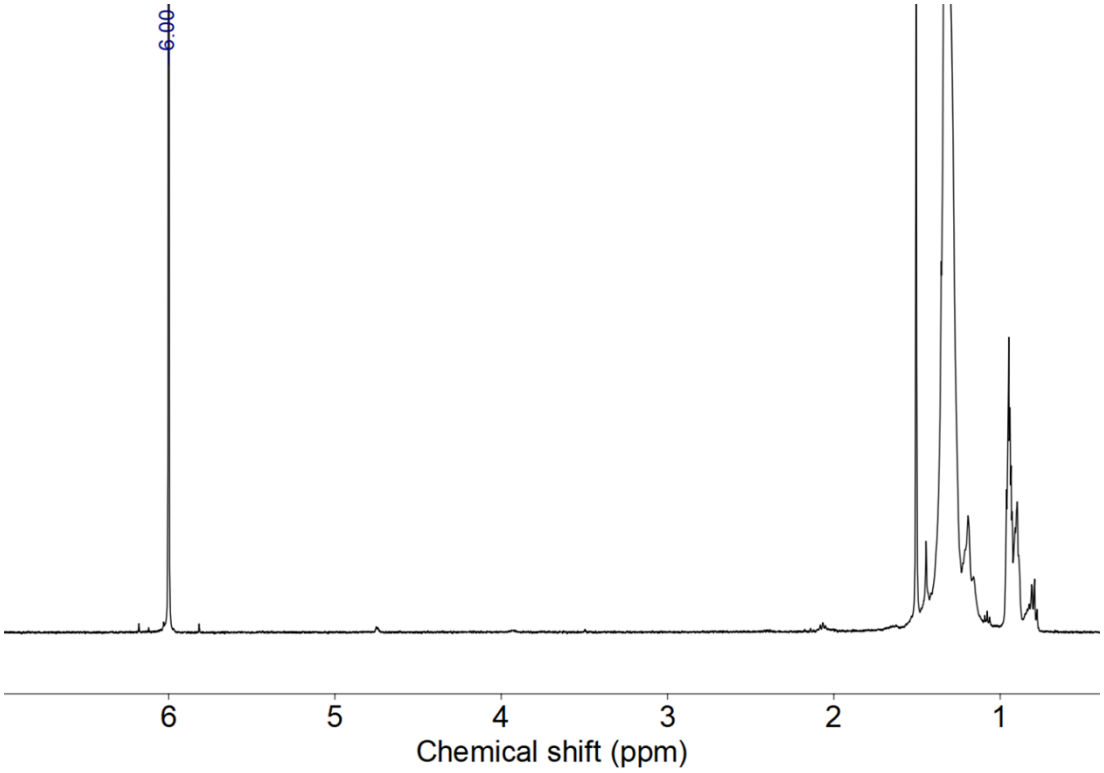

Figure S14. ^{1}H NMR spectrum ($C_2D_2Cl_4$, 80 °C) of PE product after a 24-hour reaction with 2.5 mol% NHS in TCB at 120 °C in air.

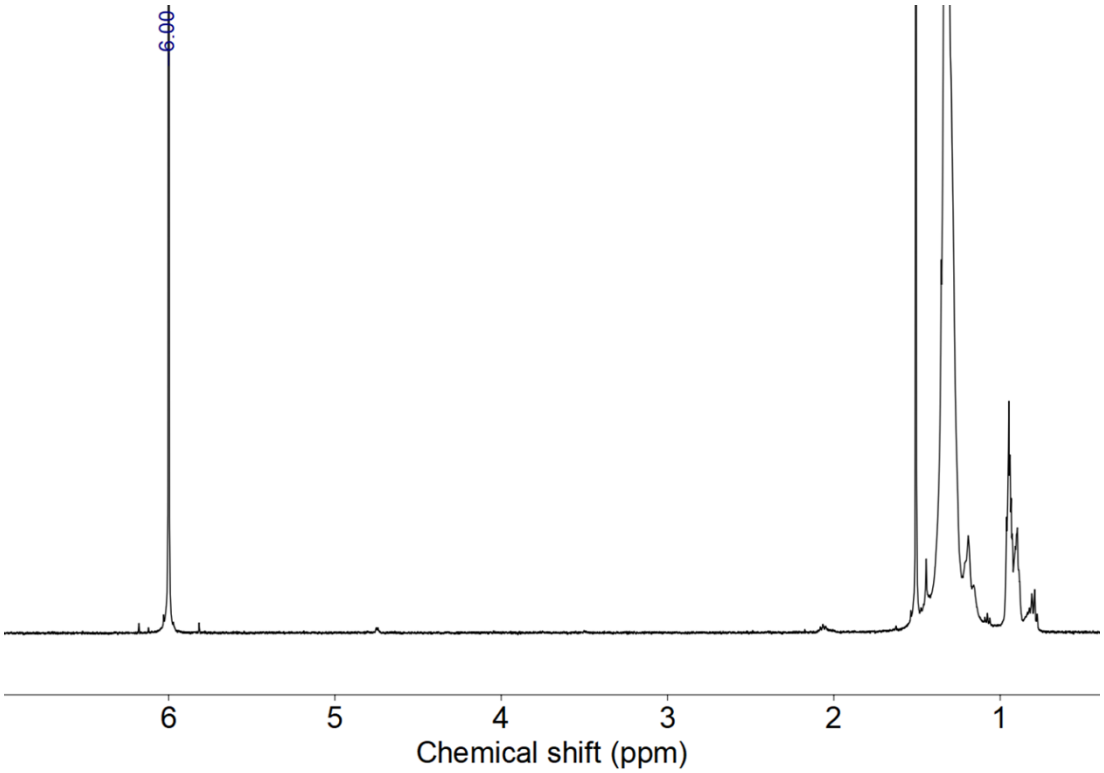

Figure S15. ^{1}H NMR spectrum ($C_2D_2Cl_4$, 80 °C) of PE product after a 24-hour reaction with 2.5 mol% TEMPO in TCB at 120 °C in air.

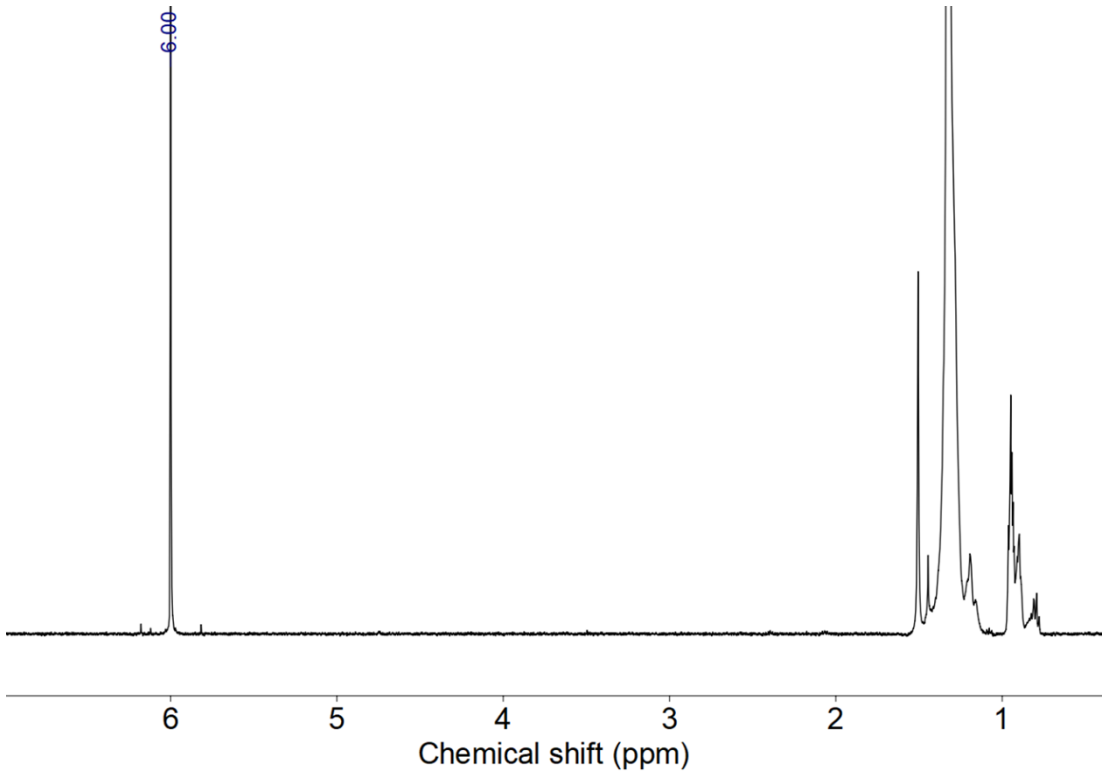

Figure S16. ^{1}H NMR spectrum ($C_2D_2Cl_4$, 80 °C) of PE product after a 24-hour reaction with 2.5 mol% HOBt in TCB at 120 °C in air.

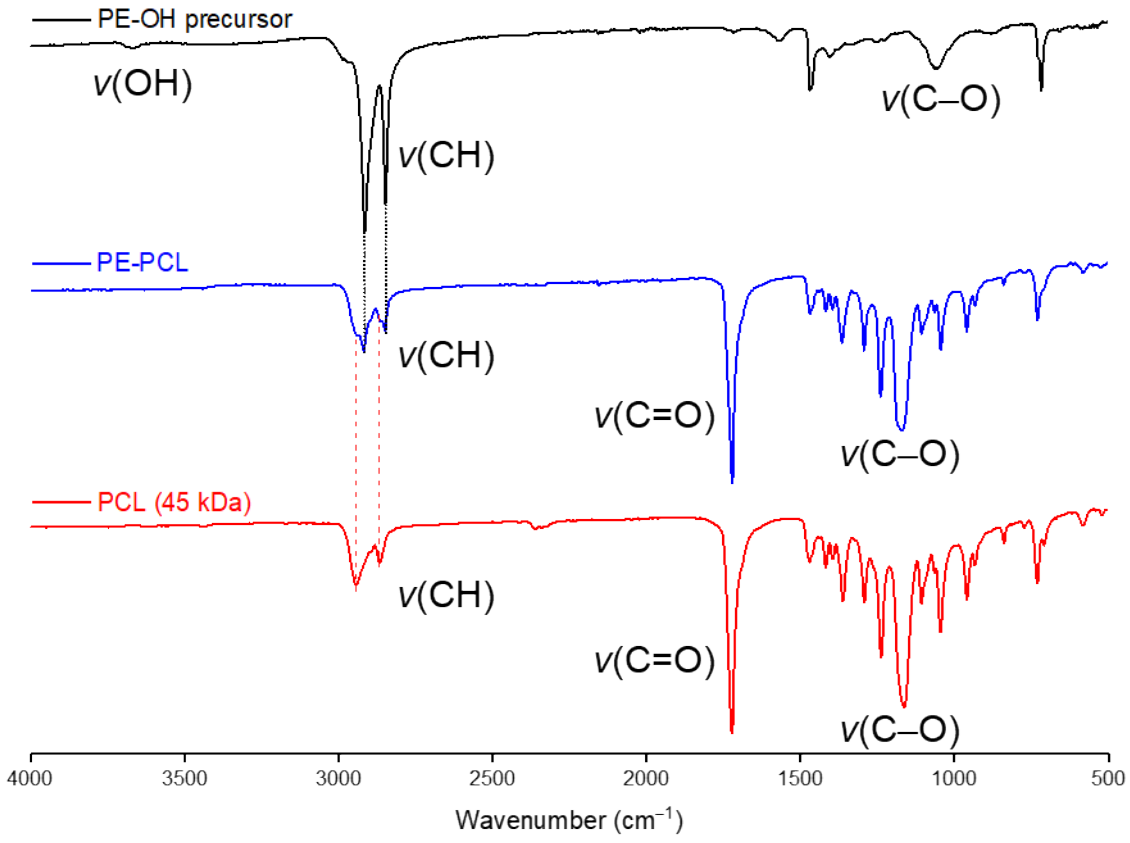

Figure S17. Stacked FTIR spectra of (top) PE-OH, (middle) PE-PCL and (bottom) pure PCL.

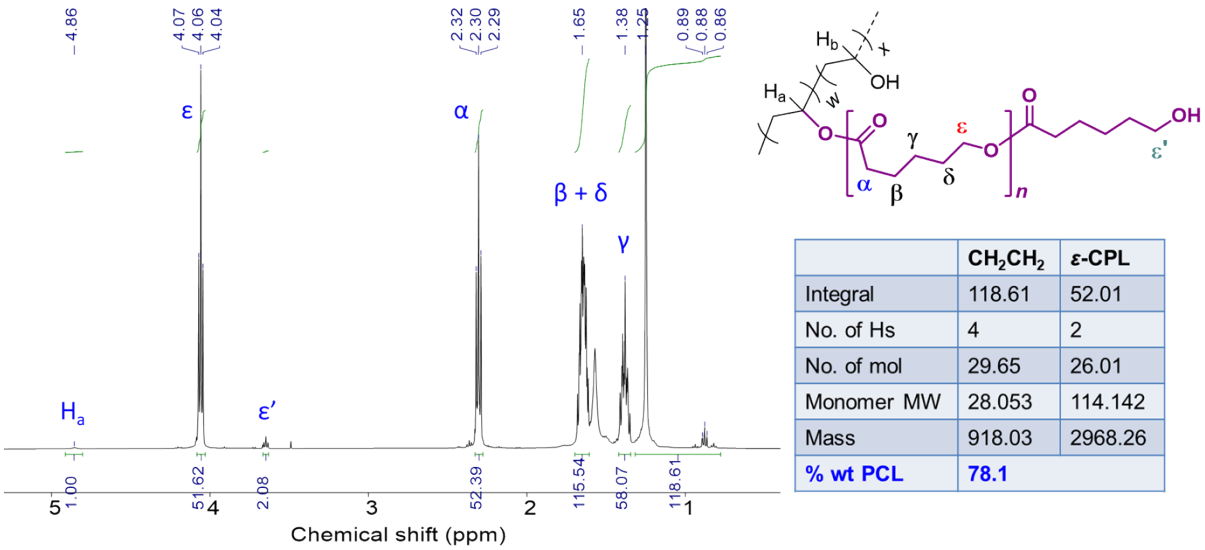

	CH_2CH_2	ε-CPL
Integral	118.61	52.01
No. of Hs	4	2
No. of mol	29.65	26.01
Monomer MW	28.053	114.142
Mass	918.03	2968.26
% wt PCL	**78.1**	

Figure S18. Integrated ^{1}H NMR spectrum ($CDCl_3$) of PE-PCL, with calculations of the mass loading of each component in the final copolymer.

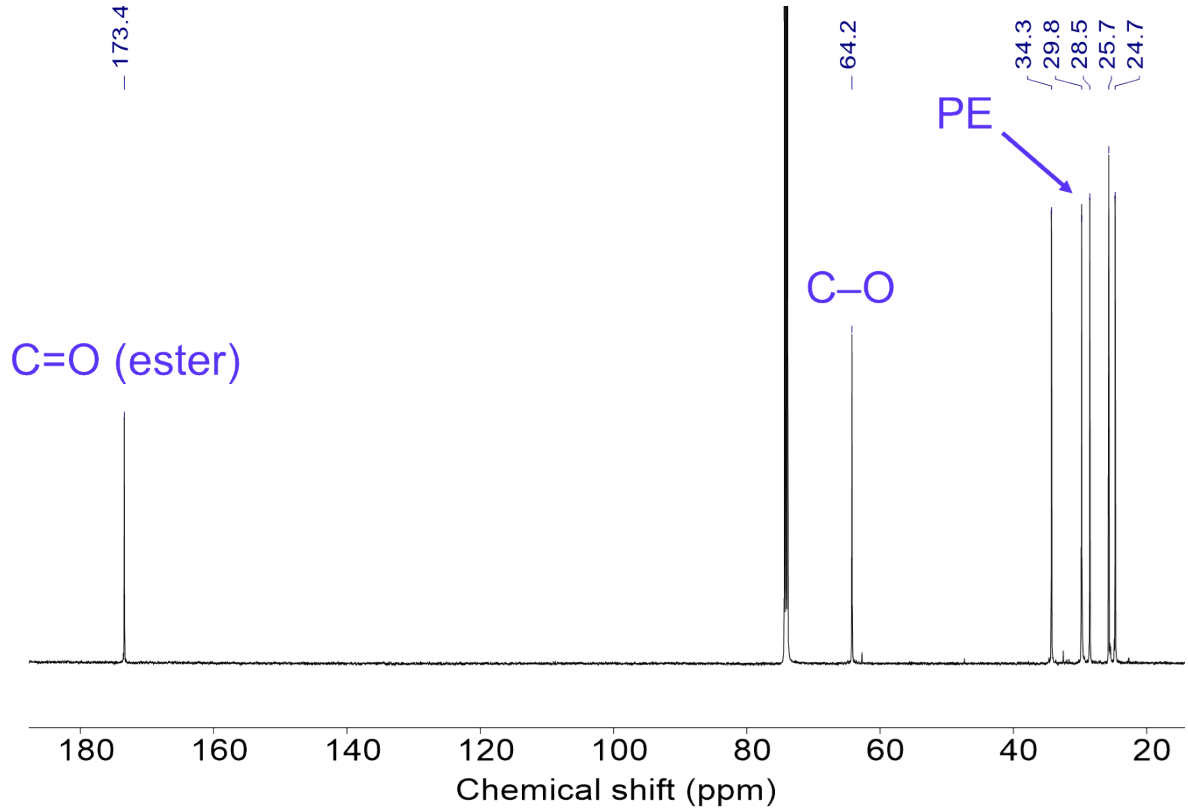

Figure S19. ^{13}C NMR spectrum ($C_2D_2Cl_4$, 80 °C) of PE-PCL copolymer.

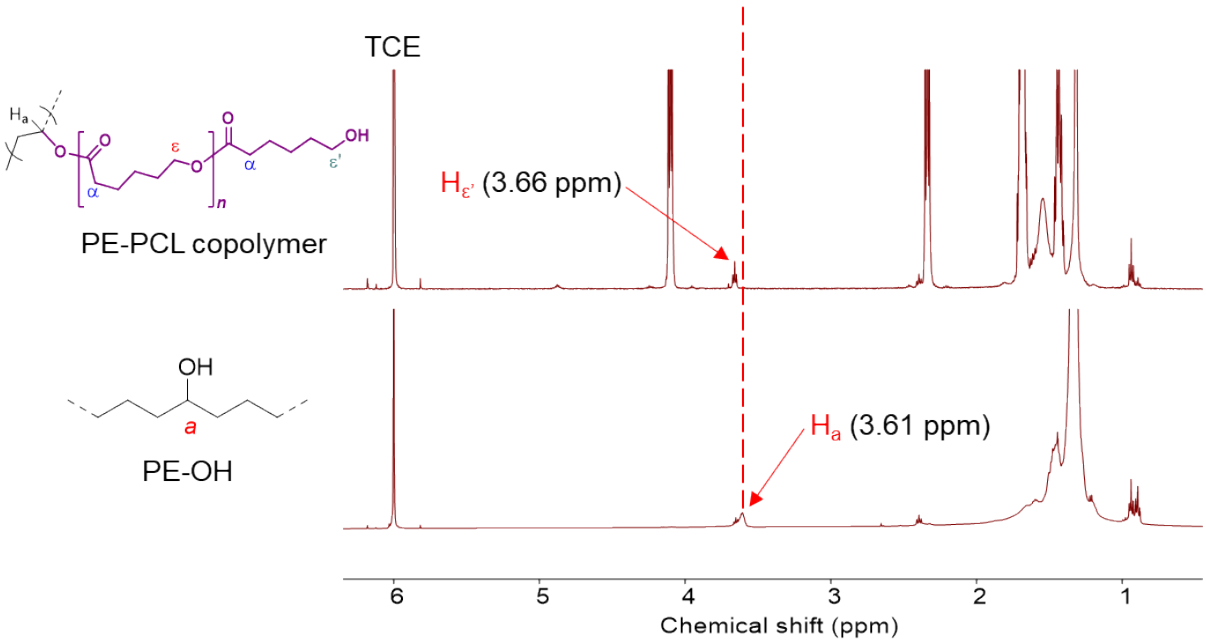

Figure S20. Stacked ^{1}H NMR ($C_2D_2Cl_4$, 80 °C) spectra of (top) PE-PCL copolymer and (bottom) PE-OH precursor.

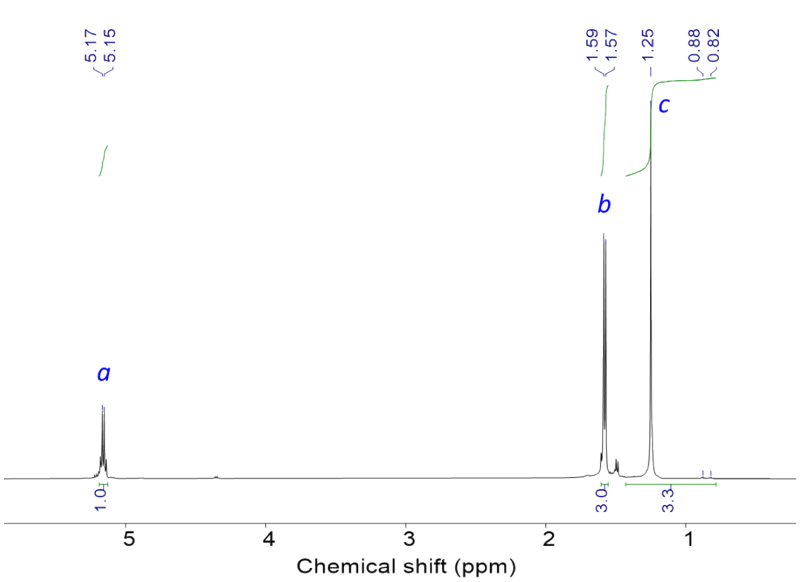

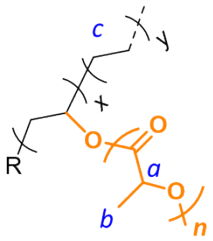

	CH_2CH_2	L-lactide
Integral	3.27	1
No. of Hs	4	2
No. of mol	0.8175	0.5
Monomer MW	28.053	144.125
Mass	22.93	72.06
% wt PLA = 75.9		

Figure S21. Integrated ^{1}H NMR spectrum ($CDCl_3$) of PE-PLA, with calculations of the mass loading of each component in the final copolymer. Note that the mass of the monomer is taken to be that of *L*-lactide rather than lactic acid, with correspondingly 2 protons per *L*-lactide repeating unit for H_a.

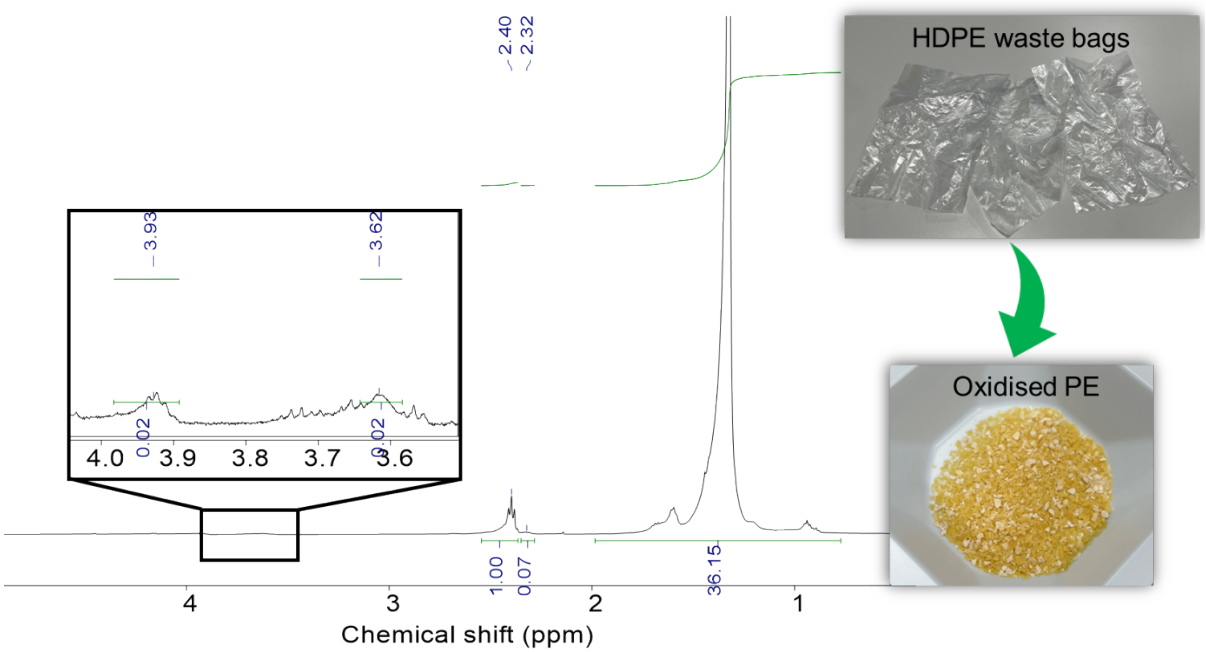

Figure S22. Oxidation of real-life HDPE waste plastic bags (inset photo) with 2.5 mol% Cl_4-NHPI in TCB at 120 °C in air for 24 h.

S3. Supporting Data for Polymer Electrolytes

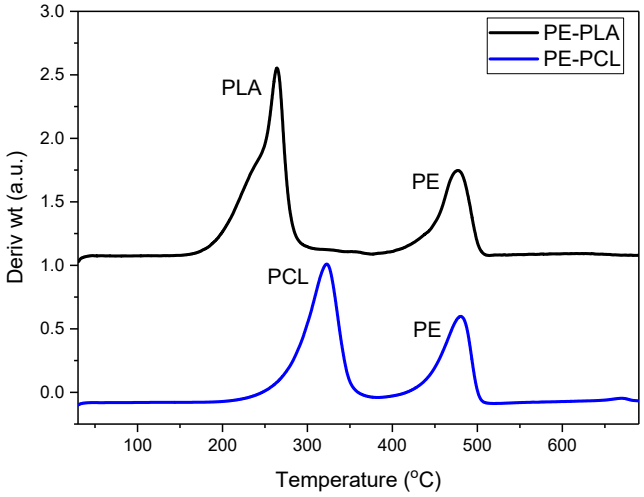

Figure S23. Stacked derivative thermogravimetric (DTG) thermal profiles of PE-PCL and PE-PLA.

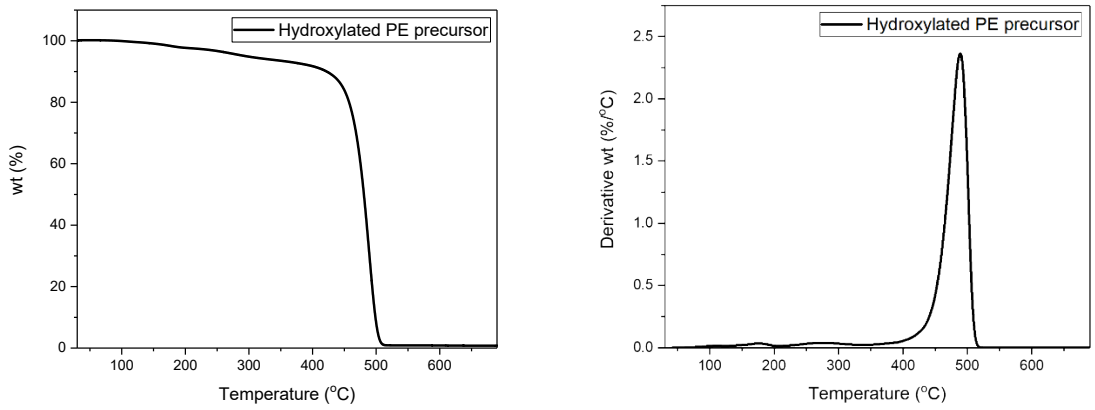

Figure S24. TGA thermogram and DTG profile of the PE-OH precursor, showing that the decomposition of the PE segments in PE-PCL/-PLA copolymers occurred ~ 490 °C.

(A)

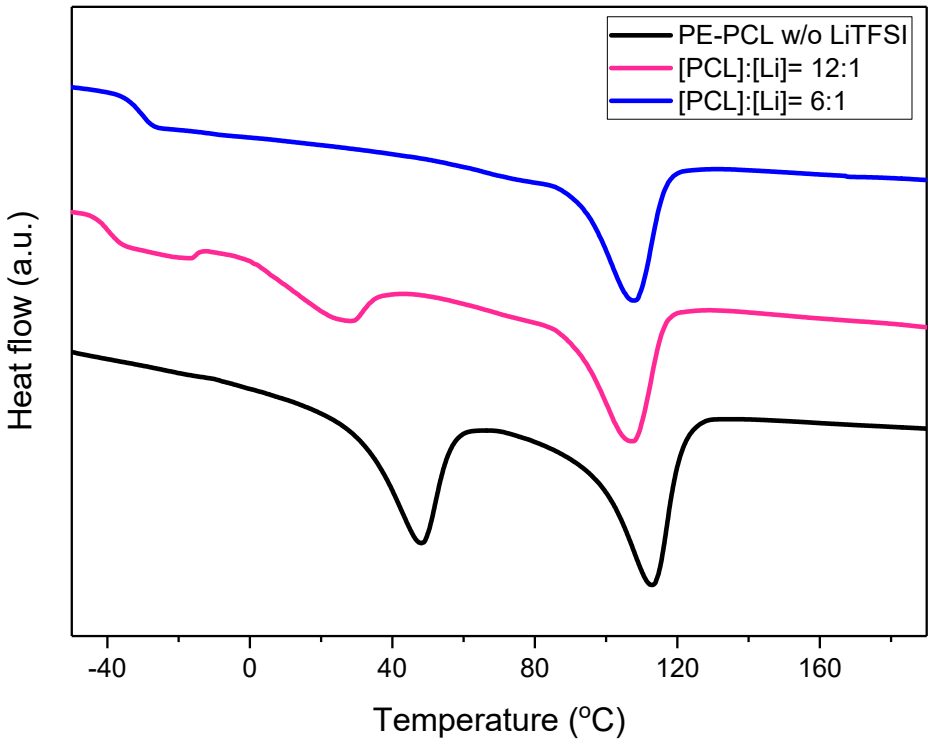
PE-PCL w/o LiTFSI
[PCL]:[Li]= 12:1
[PCL]:[Li]= 6:1
Heat flow (a.u.)
-40
0
40
80
120
160
Temperature (°C)

(B)

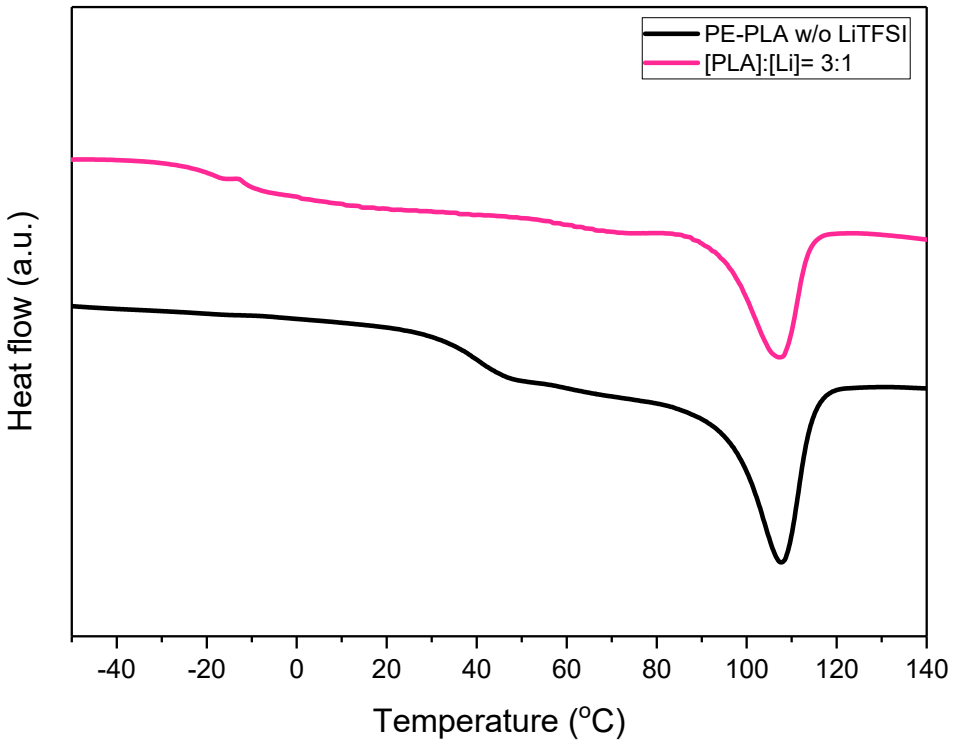
PE-PLA w/o LiTFSI
[PLA]:[Li]= 3:1
Heat flow (a.u.)
-40
-20
0
20
40
60
80
100
120
140
Temperature (°C)

	PE-PCL w/o LiTFSI	[PCL]:[Li]=12:1	[PCL]:[Li]=6:1
ΔHm (J/g)	33.3	18.6	20.0
Degree of crystallinity (%)*	11.7	6.5	7

*Degree of crystallinity χ_c is obtained by $\chi_c = \frac{\Delta Hm}{\Delta H^0 m}$ where ΔH_m= experimentally measured melting enthalpy (J/g) and ΔH^o_m = melting enthalpy of 100% crystalline HDPE (285.8 J/g).[6]

	PE-PLA w/o LiTFSI	PE-PLA [PLA]:[Li]=3:1
ΔHm (J/g)	28.0	17.3
Degree of crystallinity (%)*	19.6	12.1

*Degree of crystallinity χ_c is obtained by $\chi_c = \frac{\Delta Hm}{\Delta H^0 m}$ where ΔH_m= experimentally measured melting enthalpy (J/g) and ΔH^o_m = melting enthalpy of the α crystal of 100% crystalline PLLA (143 J/g)[7]

Figure S25. DSC thermograms of (A) PE-PCL and (B) PE-PLA with calculations of degree of crystallinity (%).

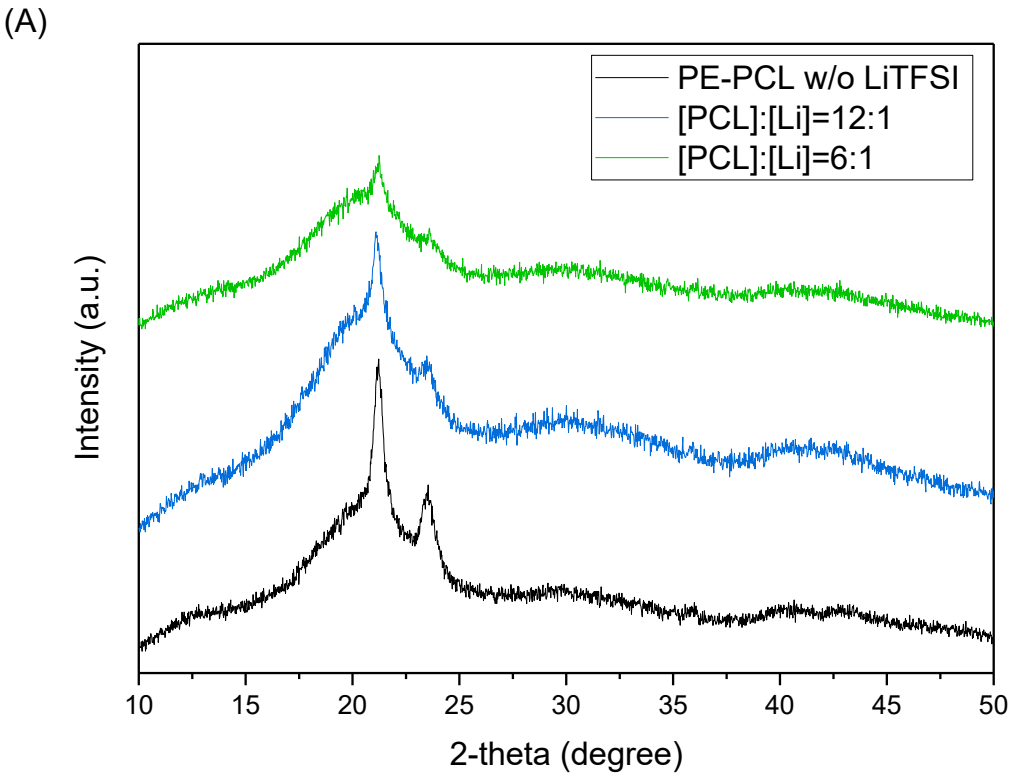

(B)

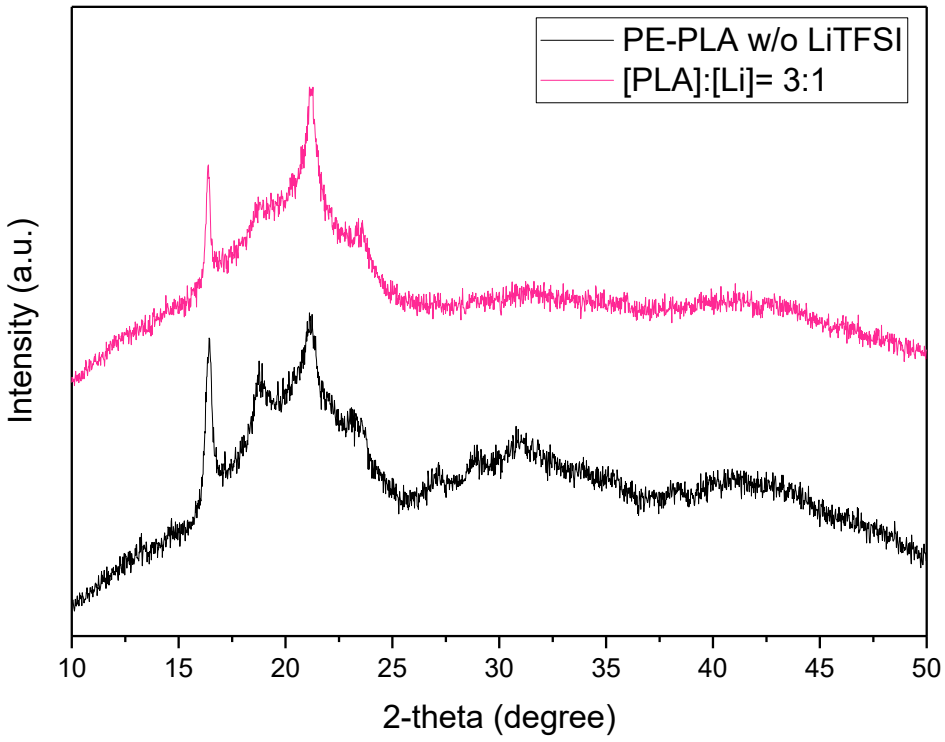

Figure S26. XRD spectra of (A) PE-PCL and (B) PE-PLA with and without LiTFSI.

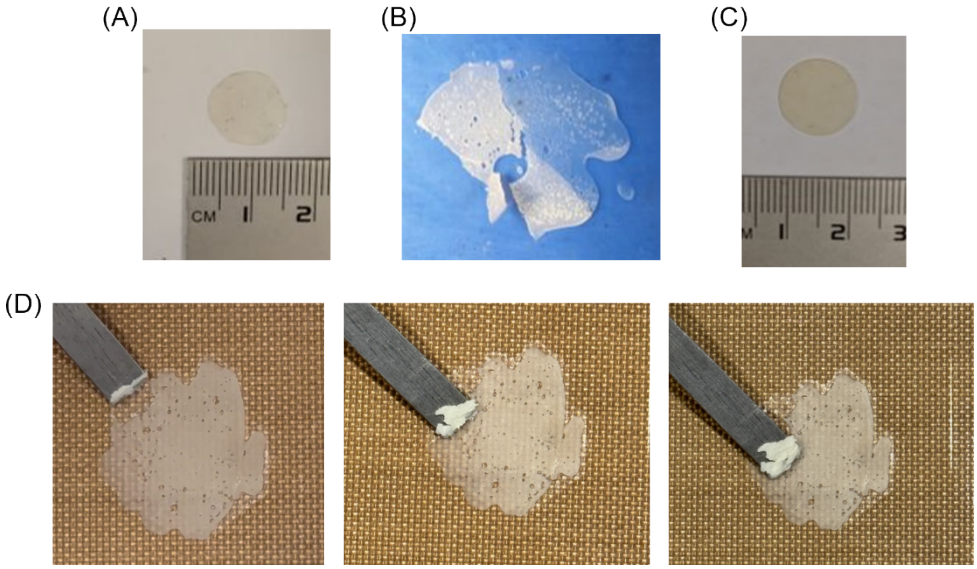

Figure S27. Optical photographs of films comprising (A) PE-PCL with [PCL]:[LiTFSI]=12:1; (B) PCL with [PCL]:[LiTFSI]=10:1; (C) PE-PCL with [PCL]:[LiTFSI]=12:1 and 22 wt% EMI-TFSI w.r.t. polymer; (D) Attempted film formation with a physical blend of PE and PCL (similar molecular weight as that used in the PE-PCL graft copolymer) with EMI-TFSI and LiTFSI ([PCL]:[LiTFSI]=12:1 40 wt% EMI-TFSI w.r.t. polymer) by hot-pressing. The blend was unable to form a free-standing film, unlike that of the covalently-grafted PE-PCL copolymer.

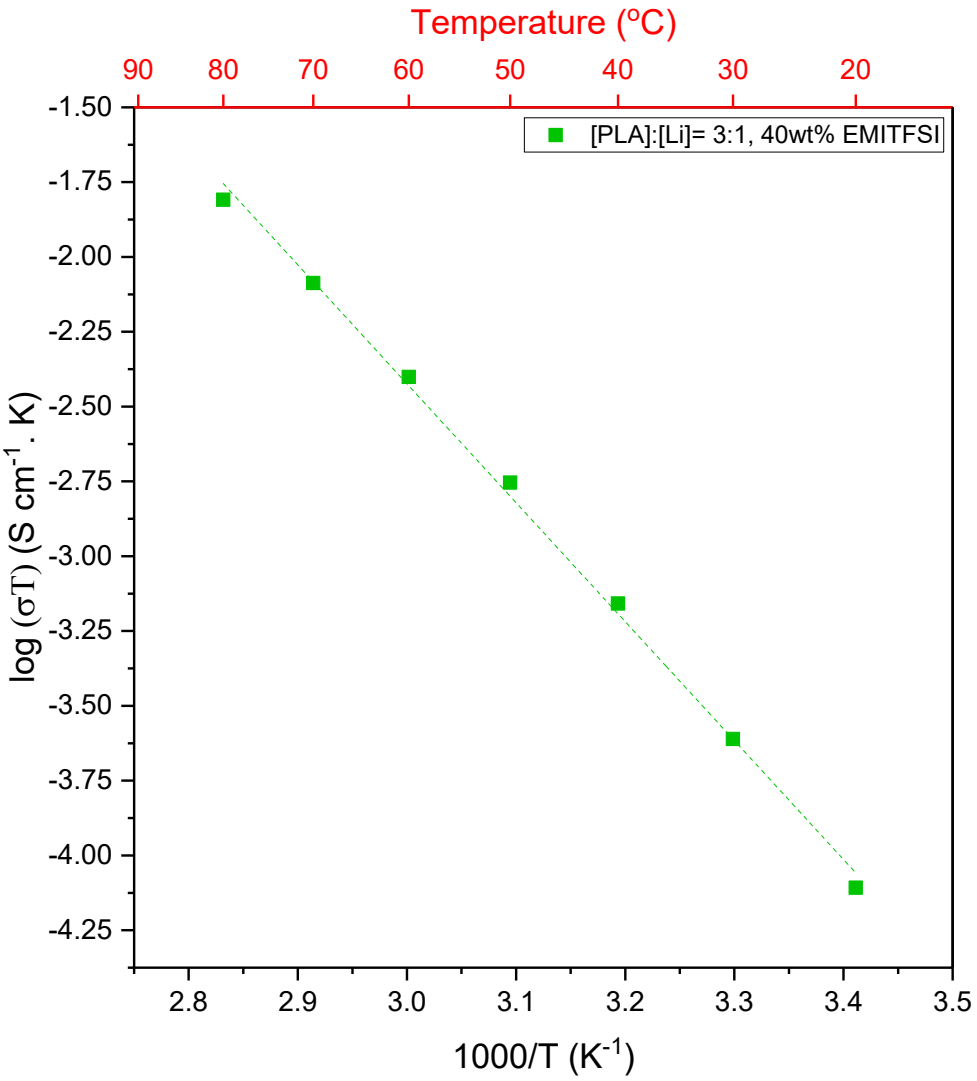

Figure S28. Effect of temperature on ionic conductivities of PE-PLA as GPEs containing LiTFSI and EMITFSI (Table 1, entry 9).

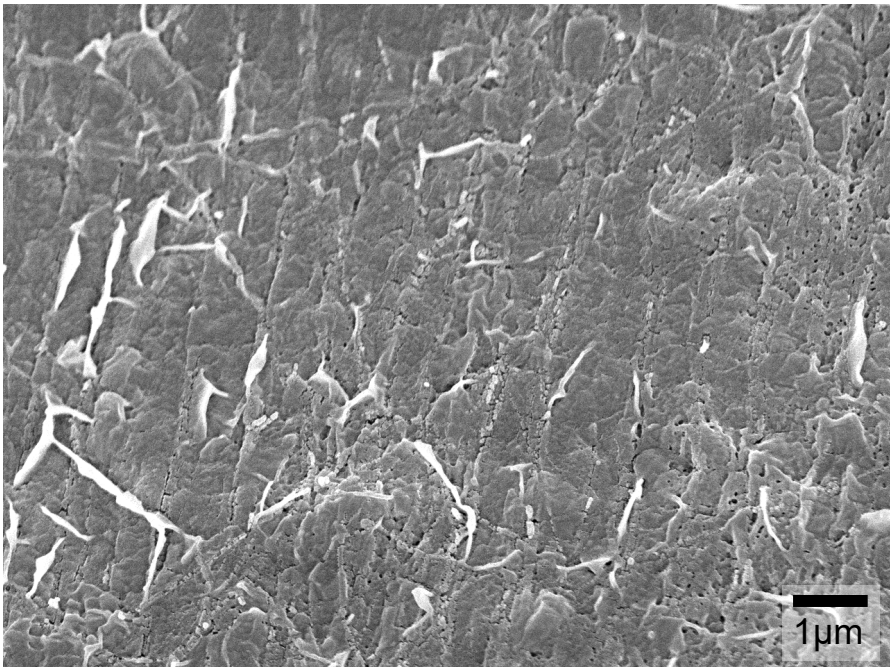

Figure S29. SEM cross-section of PE-PLA, showing tiny pores that could account for the poor ionic conductivity of the PE-PLA GPE observed. Films were dried at 90 °C for 6 h, soaked in ethanol for 6 h and dried in air before drying in vacuum oven at room temperature for 6 h. The resultant film was frozen with liquid nitrogen, fractured and imaged with SEM.

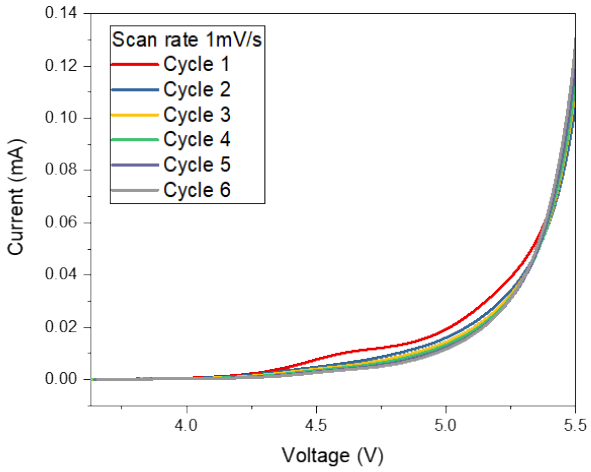

Figure S30. Linear sweep voltammetry curves of PE-PCL GPEs electrolytes at scanning rate of 1 mV/s at 60 °C (Li/PE-PCL GPE/stainless steel). There is a minor anodic peak observed initially in the first cycle which thereafter disappears as the cell stabilizes.

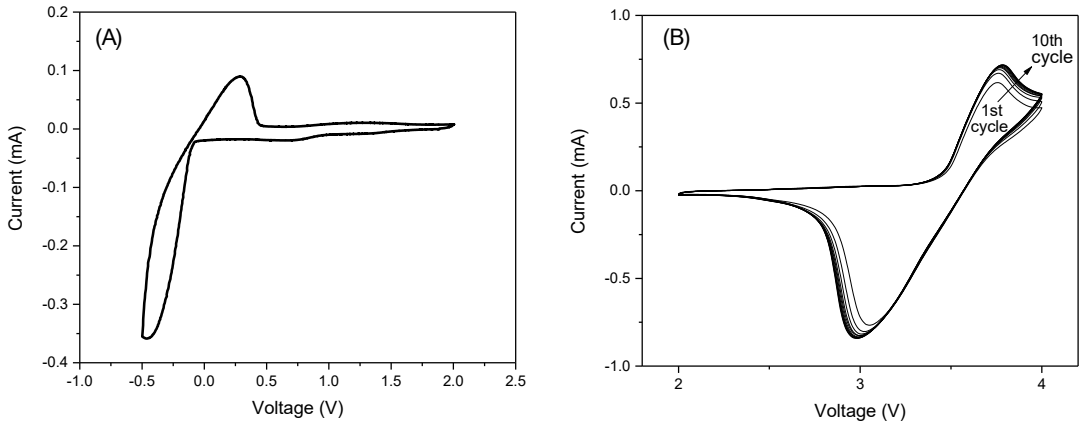

Figure S31. (A) Cyclic voltammetry of Li/PE-PCL GPE/SS at a scan rate of 1 mV/s at 60 °C and (B) Cyclic voltammetry of Li/PE-PCL GPE/LFP at a scan rate of 1 mV/s at 60 °C.

S4. Oxidative Upcycling of PE-PCL Polymer Electrolytes

Procedure for oxidative upcycling of PE-PCL SPEs

Generally, the PE-PCL SPE (117.4 mg, comprising 84.6 wt% polymer and 15.4 wt% LiTFSI) and *N*-hydroxytetrachlorophthalimide (31.0 mg, 10 mol% w.r.t. average molecular weight of PE-PCL repeating unit, i.e., 96.7 g/mol) were weighed in a 10-mL Schlenk tube. Then, acetic acid (2 mL, 10 vol% of nitric acid) was added, followed by 70% nitric acid (0.2 mL, 3 equiv. w.r.t. average molecular weight of PE-PCL repeating unit). The reaction mixture was stirred and heated to 125 °C for 24 hours in air. After the reaction has cooled to room temperature, diethyl ether (15 mL) was added to the crude reaction mixture before filtering to remove any unwanted solids. The filtrate was evaporated to dryness under reduced pressure to obtain a mixture of dicarboxylic acids. Quantification of succinic, glutaric and adipic acids was done by ^{1}H NMR analysis in DMSO-d_6 with 1,2-dichloroethane (78.8 µL, 1 mmol) added as the internal standard. LC-ESI-MS analysis was performed for identification of dicarboxylic acids present in the product mixture (Figures S30 and S31). The effect of the organocatalyst and LiTFSI on PE-PCL degradation was studied by performing two control experiments without these reagents respectively. The oxidative degradation process was also investigated on pure PCL (M_n 80 kDa) and the PE-OH precursor.

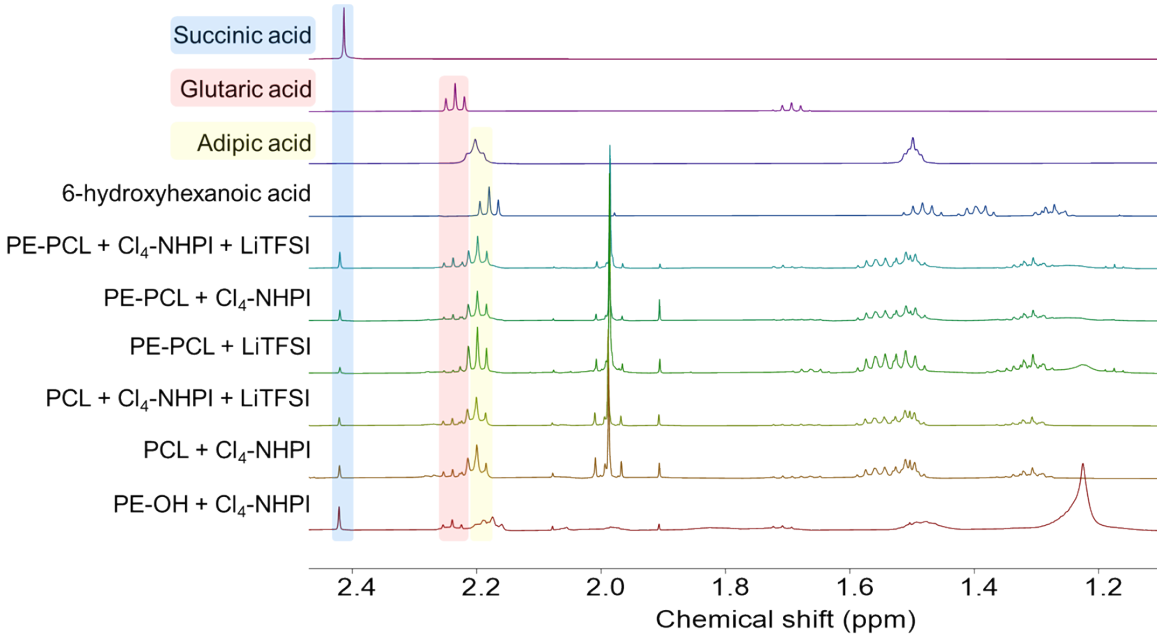

Figure S30. Stacked ^{1}H NMR spectra (DMSO-d_6) showing the presence of succinic, glutaric and adipic acids from the oxidative upcycling of polymer electrolytes (Figure 4).

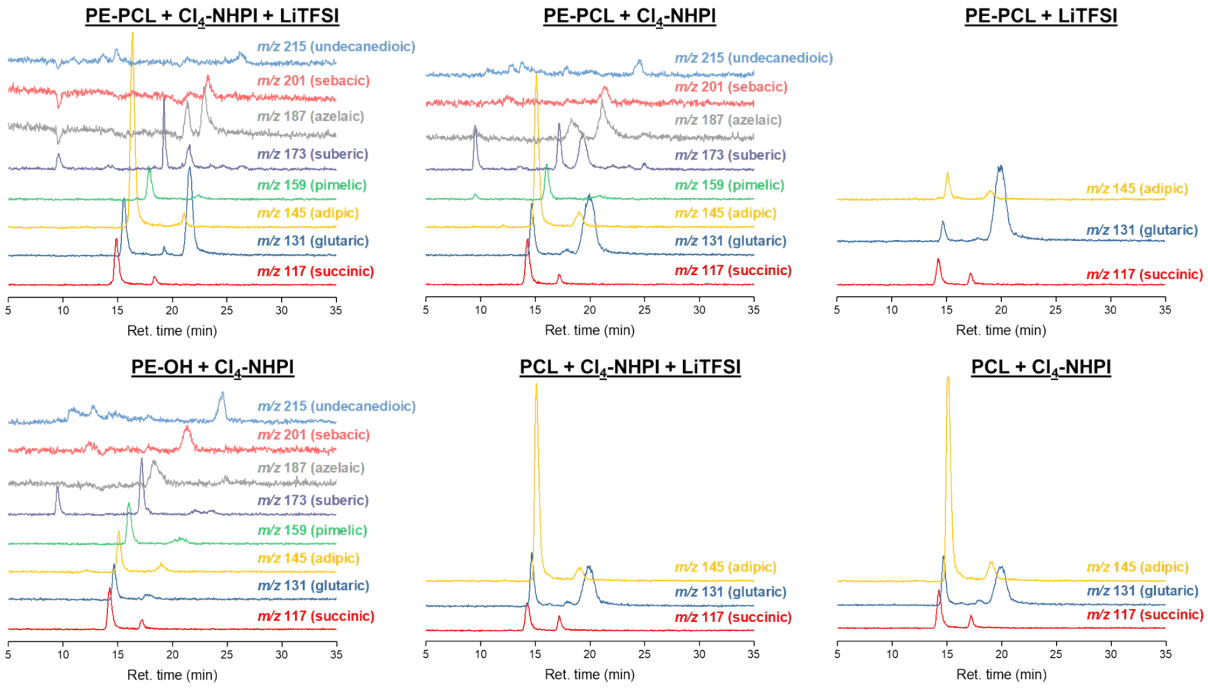

Figure S31. Extracted LC-MS traces (negative SIM mode) showing the presence of different aliphatic dicarboxylic acids formed from the oxidation of polymer electrolyte materials. Second peak (~t_R = 20 min) observed in the *m/z* 131 chromatogram may be due to 6-hydroxyhexanoic acid from oligomeric caprolactone fragmentation (not observed for PE-OH sample).

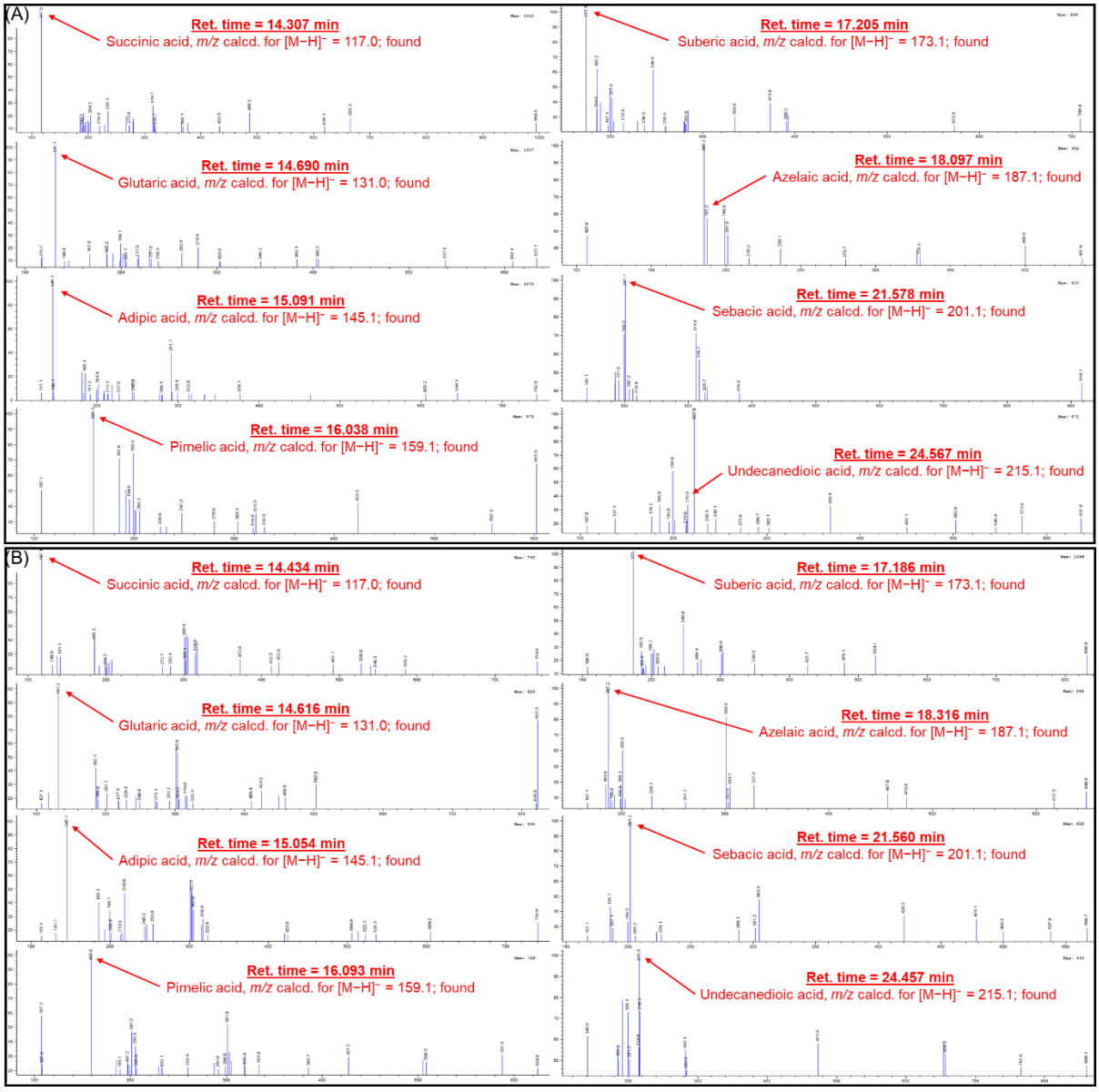

Figure S32. Negative-mode ESI-mass spectra for product obtained after reaction of (A) PE-PCL with 70% HNO_3 in AcOH at 125 °C for 24 h in the presence of Cl_4-NHPI and LiTFSI, and (B) PE-OH with 70% HNO_3 in AcOH at 125 °C for 24 h in the presence of Cl_4-NHPI.

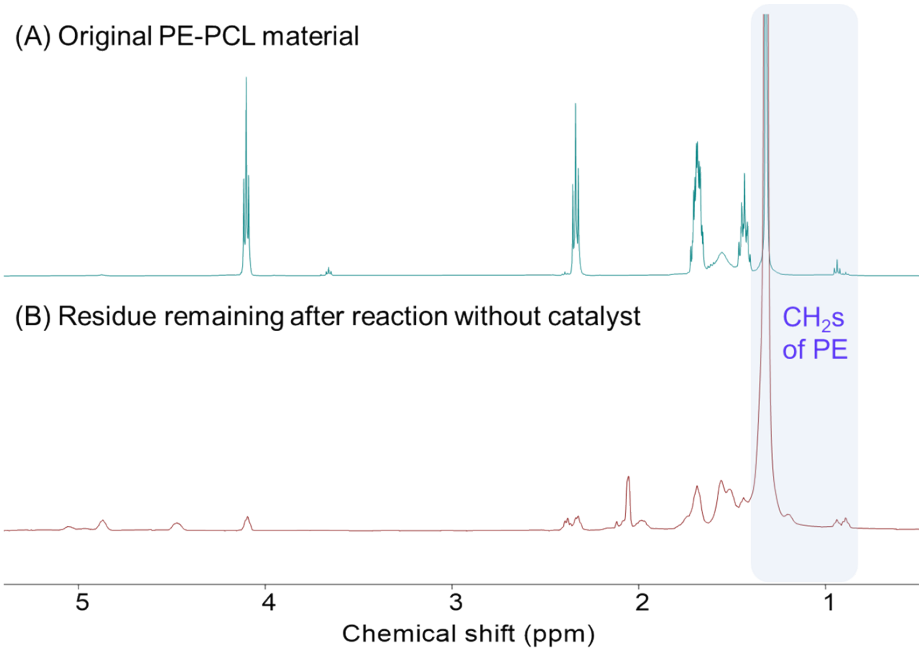

Figure S33. ^{1}H NMR spectra ($C_2D_2Cl_4$, 80 °C) of (A) the original PE-PCL polymer electrolyte *vs*. (B) the solid residue remaining after a mixture of PE-PCL and LiTFSI was reacted with 70% HNO_3 in AcOH at 125 °C for 24 h in the absence of catalyst (Figure 4 in main manuscript).

S5. References

1. M. Gardette, A. Perthue, J.-L. Gardette, T. Janecska, E. Földes, B. Pukánszky and S. Therias, *Polym. Degrad. Stab.*, 2013, **98**, 2383-2390.
2. O. Kushch, I. Hordieieva, K. Novikova, Y. Litvinov, M. Kompanets, A. Shendrik and I. Opeida, *J. Org. Chem.*, 2020, **85**, 7112-7124.
3. C. W. S. Yeung, M. H. Periayah, J. Y. Q. Teo, E. T. L. Goh, P. L. Chee, W. W. Loh, X. J. Loh, R. Lakshminarayanan and J. Y. C. Lim, *Macromolecules*, 2023, **56**, 815-823.
4. R. Amorati, M. Lucarini, V. Mugnaini, G. F. Pedulli, F. Minisci, F. Recupero, F. Fontana, P. Astolfi and L. Greci, *J. Org. Chem.*, 2003, **68**, 1747-1754.
5. F. Liang, W. Zhong, L. Xiang, L. Mao, Q. Xu, S. R. Kirk and D. Yin, *J. Catal.*, 2019, **378**, 256-269.
6. J. Zhang, V. Hirschberg and D. Rodrigue, *Recycling*, 2023, **8**.
7. M. C. Righetti, M. Gazzano, M. L. Di Lorenzo and R. Androsch, *Eur. Polym. J.*, 2015, **70**, 215-220.